WAKEMAN, BRIAN S., M.S. The Intracellular Consequences of the Interaction between Epstein Barr Virus Protein BZLF1 and the Human Protein Pax5. (2008) Directed by Dr. Amy Adamson. 61 pp.

Epstein-Barr virus (EBV) is a human herpes virus that is the cause of infectious mononucleosis and is associated with several types of cancers. These cancers include Burkitt's lymphoma, nasopharyngeal carcinoma, Hodgkin's disease, and a variety of leukemias. EBV is found in two states; latent (dormant state) and lytic (the replicating state). A protein essential for the switch and establishment of the lytic state is the immediate-early protein BZLF1. BZLF1 physically associates with a variety of host cellular proteins leading to changes in cellular environment. One such association is with the human B cell protein Pax5. Pax5 plays an important role in determining B cell differentiation as well as promoting the latent state in EBV infected cells through the activation of the EBV latent promoter Wp. I examined the BZLF1/Pax5 complex to determine if this interaction produces specific cellular changes during lytic infection including histone methylation state of chromatin during EBV infection and whether the BZLF1/Pax5 complex effects Pax5 ability to transcriptionally activate two of its target genes, CD19 and CD79a. My results showed that during lytic replication the expression of the EBV protein BZLF1 resulted in increased levels of Pax5 which resulted in increased levels of Pax5 transcriptional targets CD19 and CD79a and hypermethylation of histone-H3 lysine-9. These intracellular changes caused by BZLF1 and the increase in Pax5 may be underlying causes of cancers associated with EBV and warrant further investigation.

.

THE INTRACELLULAR CONSEQUENCES OF THE INTERACTION BETWEEN EPSTEIN BARR VIRUS PROTEIN BZLF1 AND THE HUMAN PROTEIN PAX5

By

Brian S. Wakeman

A Thesis Submitted to
the Faculty of The Graduate School at
The University of North Carolina at Greensboro
in Partial Fulfillment
of the Requirements for the Degree
Master of Science

Greensboro
2008

Approved by

_____
Committee Chair

In honor of my loving parents who have been instrumental in my success. Through the easy times and the hard their unconditional love, support, and guidance has always been there to help me along the way.

APPROVAL PAGE

This thesis has been approved by the following committee of the Faculty of The Graduated School at The University of North Carolina at Greensboro.

Committee Chair_____
Amy Adamson

Committee Members_____
Karen Katula

_____
Dennis LaJeunesse

_____
Date of Acceptance by Committee

_____
Date of Final Oral Examination

ACKNOWLEDGEMENTS

I would like to thank Dr. Adamson for all of the time, patience, and energy she has contributed to my success in completing this project. Her knowledge, work ethic, and fun nature have made my two years in her lab an incredible experience. I will forever be indebted to her for laying part of the foundation that will continue to be the basis, for hopefully, a very long scientific career.

I would also like to thank Dr. Katula and Dr. LaJeunesse for their input and support of my project, without them I would have had a hard time finishing my work. I thank them for giving me valuable ideas, as well as, allowing themselves to be sounding boards to my many rants and complaints.

Finally, I would like to thank my family and friends. They have made the last two years two of my best, without them, I would be a shell of who I am today.

TABLE OF CONTENTS

Page

LIST OF FIGURES

Page

CHAPTER I

INTRODUCTION

The Epstein Barr virus (EBV) is a human herpesvirus that infects 95% of the world's adult population. Primary infection with EBV results in infectious mononucleosis while also predisposing certain individuals to a variety of cancers. Several of the associated cancers include Burkitt's lymphoma, Hodgkin's disease, nasopharyngeal carcinoma, post-transplant lymphoproliferative disease, and certain leukemias like large granulocyte leukemia (Rickinson 2002). The widespread infection and association with a variety of cancers highlight the need for in-depth analyses of how EBV interacts with host cells.

EBV normally infects two types of cells: epithelial cells and B cells. EBV is also found in two phases, lytic and latent. EBV found in epithelial cells is undergoing lytic productive replication while EBV found in B cells initially replicates in a lytic manner and then enters a latent dormant state. B cells appear to be the primary target for EBV infection. Under normal circumstances, B cells differentiate into plasma cells where they will secrete Ig, or memory B cells (Calame, et al. 2003). EBV takes advantage of this differential pathway allowing the virus to replicate while also immortalizing the cells allowing EBV to be carried throughout the lifetime of the host (Rickinson, 2002). Through the lifetime of infection, EBV in B cells exists in the latent phase, and

during latent infection there is minimal expression of viral genes. However, under certain conditions like immune suppression, the latent virus within B cells may switch back to the lytic mode of replication (Rickinson, 2002).

To initiate lytic replication there is a cascade of EBV genes that become expressed. The first genes expressed during lytic phase are the immediate-early genes, BZLF1 and BRLF1. These genes act as transcription factors that bind to and activate the promoters of early EBV genes, setting off a cascade of lytic gene transcription (Chevallier-Greco et al 1986; Kenney et al 1989; Giot et al 1991; Quinlivan et al. 1993; Rickinson 2002). The early genes encode viral proteins required for viral DNA replication. DNA replication is followed by EBV late-gene expression and packaging of the new virus (Rickinson 2002). The immediate-early genes are essential for the activation of the EBV early gene expression. Loss in the function of BZLF1, such as in the BZLF1 mutant Z311, halts EBV lytic replication (Giot et al. 1991). The dependency of EBV early genes on the BZLF1 protein is so crucial that even a mutation in a single amino acid residue results in the inability to activate the lytic cycle (Schelcher 2005).

Since EBV replication is dependent on the host cell's environment, BZLF1 and other immediate-early EBV proteins will interact with and alter functions of cellular proteins, thus altering the cellular environment to provide optimal conditions for the virus. These proteins induce changes in the host cell through modulation of cell cycle progression, transcriptional functions, gene silencing, as well as others mechanisms. BZLF1 specifically has been shown to interact with and modify the function of many

known cellular proteins (Adamson et al. 2005; Adamson and Kenney, 2001; Adamson and Kenney, 1999; Adamson et al. 2000).

It is clear, by looking closely at cellular proteins, that EBV proteins manipulate the host cell to maintain an optimal environment for viral replication. Physical interaction between viral proteins and cellular proteins is a major component in producing the changes observed in EBV infected cells. BZLF1 has been shown to physically associate with the p53 protein. p53 is essential for the regulation of cell apoptosis and checkpoint control, and overexpression of p53 results in the loss of BZLF1's ability to activate EBV early promoters. Interactions with BZLF1 resulted in p53 losing its ability to activate p53 response promoters (Zhang et al 1994). BZLF1, by physically associating with p53, allows the host cell to be manipulated in a way that promotes lytic replication.

The protein CBP also physically associates with BZLF1, while localizing to mitotic chromosomes and this interaction leads to an increase in BZLF1's ability to activate EBV early genes (Adamson and Kenney 1999). CBP is a histone acetylase that acts to acetylate histones in chromatin, and histone acetylation associated with gene expression. CBP localized to mitotic chromosomes in the presence of BZLF1 resulted in significantly increased histone acetylation levels, which indicated CBP remains functional and alters the normal chromosome state (Adamson 2005). Besides p53 and CREB-binding protein (CBP), BZLF1 has shown association with promyelocytic leukemia protein (PML), c-Jun N-terminal kinases, and p38. (Adamson et al 2000; Adamson and Kenney 2001; Adamson et al. 2005).

An important protein that has recently been found to interact with BZLF1 is the human protein Pax5. This BZLF1/Pax5 interaction was discovered through an unconventional route of screening for BZLF1 genetic interactions in Drosophila. Through a genetic screen, it was determined that BZLF1 inhibited the function but not the expression of Drosophila *shaven*, a Pax5 homolog (Adamson et al, 2005). In addition to a genetic interaction BZLF1 also physically associates with human Pax5. The Pax5/BZLF1 complex was still able to bind to a consensus Pax5 DNA binding site, but was not able to promote transcription efficiently (Adamson et al, 2005).

Pax5 is an essential protein involved in promoting B cell differentiation and inhibiting the formation of other cell lineages (Enver, 1999). Pax5 the protein is a transcription factor and is an essential early activator of B cell differentiation, committing cells to a B cell fate. Pax5 contains a novel, highly conserved DNA-binding motif, known as a paired box domain. Loss of Pax5 leaves cells stalled at a point before differentiation, and these cells may be converted to other cell lineages such as T cells, granulocytes, macrophages, and natural killer cells.

Pax5 induces cells to commit to a B cell fate by promoting V_H to D_HJ_H gene rearrangement. Pax5 promotes V_H to D_HJ_H gene arrangement through the loss of histone-H3 lysine-9 methylation in the V_H locus. (Johnson et al. 2004). These demethylated histones become part of the recombination signal sequence (Johnson et al. 2004). The recombination activating proteins RAG-1 and RAG-2 will recognize and perform the first cleavage of the DNA containing recombination signal sequences (Kishi et al. 2000). The cleavage and joining of genes is what allows for the diverse array of immunoglobulin

receptors found on B cells. Loss of RAG-1 or RAG-2 results in the inability of B cells to develop properly. Besides the promotion of V_H to D_HJ_H gene arrangement, Pax5 has also been linked to transcriptional activation of RAG-2 expression (Johnson et al. 2004)

Pax5 also transactivates the B-cell specific genes *CD19*, *blk*, *CD79a*, and *RAG-2* (Figure 1). Pax5 also represses the genes *perforin*, *GATA-1*, *M-CSF-R*, and *Notch1* (Figure 1). CD19 is a cell surface protein that functions to define signaling thresholds for cell surface receptors, which are responsible for B lymphocyte selection, activation, and differentiation (Engel et al. 1995). Blk is protein tyrosine kinases of the src family and physically associates with the B cell antigen receptor complex (Burkhardt at al. 1991). CD79a is a protein that functions to transmit a signal after antigen binding. It is found to physically associate with immunoglobulin in the cell membrane of B cells (Mason et al. 1995).

To look more closely at how EBV may manipulate the infected cell environment, I investigated the effect BZLF1 interaction with Pax5 has on the host cell. BZLF1 physically interacts with Pax5, localizes Pax5 to mitotic chromosomes, and stabilizes the Pax5 protein (Adamson 2005; Adamson et al. 2005). This physical interaction leads to widespread changes within an infected cell. Since Pax5 is necessary for cells to commit to a B cell fate and activates the expression and repression of several genes, any changes to Pax5 transcriptional activity may be detrimental to cellular integrity. Pax5 also plays an important role in lytic to latent viral activity. Pax5 aids in the establishment of EBV latency in infected B cells by activating the latent promoter Wp. Wp is the first latent promoter activated when EBV switches between lytic and latent replication, and Wp will

activate the early EBV transcription factors EBNA2 and EBNA-LP (Tierney et al 2000). The physical association between the lytic-associated BZLF1 and Pax5 may aid in the establishment or prolonging of lytic replication by repressing the ability of Pax5 to activate the latent promoter Wp.

	Genes			Function In
Genes Repressed by Pax5 in B Cells	*Ccl3*(MIP-1α;S)	*Ccl9*(MIPY;S)	*Ccr2* (R)	
	Ccr5 (R)	*Itgal*(LFA-1; R)	*Cd47* (IAP,R)	
	Tspan7 (Tm4sf2;R)	*Emb* (Embigin; R)	*Vav3* (ST)	**Adhesion, Migration**
	Igf2 (S)	***Flt3*** (Flk2; R)	*Ly6a*(Sca1;R)	**Progenitors**
	Tnsf11(OPGL; S)	***Csf1r*** (M-CSFR; R)	*Lilrb4* (Gp49b; R)	
	Cd33 (Siglec-3; R)	*Ramp1* (CGRP-R;R)	*Fcer1g* (FcR-γ;R)	
	Grap2 (Mona; ST)	*Lat2* (NTAL; ST)	*Lmo2* (TF)	**Myeloid cells**
	Notch1 (R, TF)	*Tcrd* (R)	*Cd28* (R)	
	Grap2 (Mona; ST)	*Ppp3ca* (CnA-α; ST)	*Lck* (ST)	
	Satb1 (TF)			**T Cells**
	Igj (J-chain; S)	*Sdc1* (CD138; R)	*Prdm1* (Blimp1; TF)	**Plasma Cells**
Activated Genes	***Cd19*** (R)	*Cr2* (CD21; R)	***Fcer2a*** (CD23; R)	
	Cd40 (R)	***Cd72*** (R)	***Cd79a*** (Igα; R)	
	Blnk (SLP65; ST)	***Ebf1*** (TF)	*Lef1* (TF)	
	C2ta (CIITA; TF)	*Aicda* (AID)		**B Cells**

Figure 1: Pax5 dependent gene expression. A listing of Pax5 transcriptional targets grouped by repression (yellow) or activation (blue) within differing cell types. Proteins encoded by given genes are found in parenthesis. Bold-faced genes are genes known to be direct targets of Pax5. Overall a total of 42 genes are listed, demonstrating the multifunctional nature of Pax5 (Cobaleda 2007).

Like the other BZLF1 associated protein CBP, Pax5 utilizes epigenetic mechanisms as it acts to demethylate histone-H3 lysine-9 to promote V_H to D_HJ_H gene arrangement. If Pax5 retains its ability to affect histone methylation levels, its physical interaction with BZLF1 could possibly lead to cell-wide epigenetic changes. Epigenetic effects to chromatin structure are important to classify, as they often are associated with a wide variety of cancers. Specifically, histone-H3 lysine-9 methylation is associated with gene silencing in cancer cells (Nguyen et al. 2002). In addition, some gene silencing has been linked to cancers associated with EBV. The gene promoter of p73, a tumor suppressor, is methylated in gastric carcinoma only when in association with EBV (Ushiku et al. 2006). This association between epigenetic marks, cancer, and EBV promotes the need for an in-depth examination of any possible mechanisms leading to chromatin changes.

My goals of this study were to identify the consequences of the BZLF1/Pax5 interaction. I showed that the BZLF1/Pax5 physical interaction leads to a stabilization and consequently large increase in Pax5 protein levels within infected cells. I also demonstrated the effect BZLF1 and Pax5 have on the methylation state of chromatin in BZLF1 expressing cells. Finally, I showed what changes occur in the expression levels of Pax5 transcriptional targets CD19 and CD79a in EBV infected cells.

Specific Aims:

1. Determine the status of Pax5 expression levels in B cells before, during, and after EBV infection.
2. Determine if changes in Pax5 protein are due to changes in Pax5 mRNA levels
3. Examine the histone methylation state of chromatin in BZLF1-expressing and EBV infected B cells
4. Examine the protein levels of Pax5 transcriptional targets CD19 and CD79a in BZLF1-expressing and EBV-infected B cells.

CHAPTER II

MATERIALS AND METHODS

Cell Lines: Raji cells are an EBV-positive Burkitt's lymphoma line. They were maintained in HyQ RPMI 1640 media with 10% fetal bovine serum as well as fungal and bacterial inhibitors (50µl/500ml streptomycin, 50µl/500ml penicillin, 0.25ug/ml amphotericin B). HeLa cells, a cervical carcinoma line, and D98/HE-R1 cells, an epithelial cell line formed by the fusion of a HeLa subclone with the EBV positive Burkitt's lymphoma line P3HR/1, were maintained in DMEM media with 10% fetal bovine serum as well as fungal and bacterial inhibitors (Glaser and O'Neill 1972).

Plasmids: The control vector was SVpIE which contained the SV40 enhancer element. The BZLF1 expression vector was the BZLF1 gene in the SVpIE vector, and the Pax5 expression vector contained the human Pax5 cDNA downstream of the CMV promoter in the EVRF2 vector.

Transfections: D98/HE-R1 and HeLa transfections were performed by the calcium phosphate method (Sambrook et al. 1989). Briefly, cells were counted and plated. Then 5µg of DNA for each condition, vector, BZLF1 alone, Pax5 alone, and BZLF1 + Pax5, were mixed with 0.1x TE. This was then mixed with 2xHBS, and 2M

$CaCl_2$. This DNA mixture was added drop wise to the plated cells. Cells were incubated overnight at 37˚C, washed with 1x PBS, and incubated for another 24 hours in DMEM media.

Raji cells were transfected using electroporation. Cells were counted and resuspended in 0.8ml RPMI 1640 media. 5µg of DNA for each condition, vector or BZLF1, was added to the cells. Electroporation was performed with a Zapper electroporation unit (BioRad) at 350 volts, 950uF for 2 seconds. All transfections were then transferred to 10ml RPMI 1640 media for 48 hours

Infection of Cells with EBV: Raji cells were infected with 2ml of the viral strain EBfaV-GFP in a suspension of $2x10^5$ cells in the presence of TPA (12-O-tetradecanoylphorbol-13-acetate, 20ng/ml) and BA (butyric acid, 3mM) for 1 hour at 37˚C with vigorous shaking. Cells were then centrifuged, the supernant discarded, and resuspended in fresh complete RPMI 1640 medium (Speck and Longnecker 1999).

Immunocytochemistry for Pax5: Cells were washed with 1x PBS and fixed for 15 minutes using 1ml 4% paraformaldehyde in 1x PBS. 500µl incubation mix was added, consisting of 1x PBS, 5% donkey serum, and 0.1% Triton X. Cells were then washed with 1x PBS and 50µl of the primary antibody Pax5 (Santa Cruz) at a dilution of 1:100 was added. Cells were incubated for 1 hour at 37˚C, washed with 1x PBS and 50µl of diluted secondary antibody [donkey anti-goat-CY3 (Jackson ImmunoResearch) at a dilution of 1:200] was added. After incubating 1 hour at 37˚C in the dark, cells were

washed with 1x PBS, stained with Hoechst stain at a dilution of 1:2000, and mounted in antifade media (DakoCytomation).

Immunocytochemistry for H3K9 and Z: Cells were washed with 1x PBS and fixed for 15 minutes using 1ml 4% paraformaldehyde in 1x PBS. Cells were incubated in 1x PBS containing 0.25% Triton X. Cells were then blocked for 30 minutes in 1% BSA in PBST consisting of 1x PBS, 0.1% Triton X, and 1% BSA (Bovine Serum Albumin; Sigma). Cells were then incubated in 50µl diluted primary antibody anti-H3K9 (Abcam) at a dilution of 1:5000 and anti-BZLF1 (Argene) at a dilution of 1:100, for 1 hour at 37˚C. Cells were washed with 1x PBS then incubated for 1 hour at 37˚C in 50µl diluted secondary antibody [donkey anti-rabbit-CY3 (Jackson ImmunoResearch) at a dilution of 1:200 and donkey anti-mouse-FITC (Jackson ImmunoResearch) at a dilution of 1:200]. Cells were then washed with 1x PBS, stained with Hoechst stain at a dilution of 1:1,000,000, and mounted with antifade media (DakoCytomation)

Immunocytochemistry for CD19 and CD79a: Cells were washed with 1x PBS and fixed for 15 minutes using 1ml 4% paraformaldehyde in 1x PBS. The cell staining procedure followed the same details as immunocytochemistry of Pax5, only differing in the incubation mix components (1x PBS, 5% goat serum, 0.3% BSA,) and use of primary antibodies. Primary antibodies [anti-CD19 and anti-CD79a (Santa Cruz), as well as anti-BZLF1 (Argene)] were used at a dilution of 1:200. Secondary antibodies, DNA staining, and cell mounting remained the same.

RNA Extraction and Purification: RNA for RT-PCR was extracted and purified using a Qiagen RNeasy Mini Kit following the procedure outlined in the accompanying handbook. Briefly, cells were counted, pelleted, and RLT buffer containing β-mercaproethanol was then added. Cells were homogenized using a 20-gauge needle, and 70% ethanol added. Buffer RW1 was added, buffer RPE was then added twice, while collecting cells after each addition. Finally RNase-free water was added to collect and suspend the purified RNA. Purified RNA was quantified using a nanodrop spectrophotometer.

RT-PCR: RT-PCR was performed using a Promega Access RT-PCR System following the procedure outlined in the accompanying handbook. Briefly, 0.1u/µl AMV-RT, 0.1u/µl T*fl* DNA polymerase, 1x AMV/Tfl Reaction Buffer, .2mM dNTP mix, 1mM MgSO4, and RNA template (100 ng each) were mixed together. 1µM Upstream Pax5 5' end primer ATGGATTTAGAGAAAAATTATCCG and 1µM downstream Pax5 3' end primer TCAGTGACGGTCATAGGCAGTGGC were added (MWG-Biotech). PCR was run using first strand cDNA synthesis cycle conditions of 1 cycle 45˚C for 45 minutes, 1 cycle 94˚C for 2 minutes. Second strand synthesis and PCR amplification cycle conditions of 40 cycles of 94˚C for 30 seconds, 60˚C for 1 minute, and 68˚C for 2 minutes were used.

Protein Preparation: Cells were washed and lysed in ELB buffer (0.25M NaCl, 0.1% NP-40, 50mM HEPES [pH7], 5 mM EDTA, protease inhibitors). Extracts were

frozen/thawed two times and centrifuged. Protein concentrations were determined by performing the Bradford assay with a spectrophotometer set at OD595.

Nuclear Protein Extract: Cells were spun and washed in 1x PBS, and the liquid discarded. Cells were then resuspended in CE buffer (10mM HEPES, 60mM KCl, 1mM EDTA, 1mM DTT, 0.075% NP-40, protease inhibitors) and incubated on ice for 4 minutes. Liquid was discarded and cells resuspended in CW buffer (10mM HEPES, 60mM KCl, 1mM EDTA, 1mM DTT, protease inhibitors). Liquid was discarded and cells resuspended in NE buffer (20mM Tris/HCl, 420mM NaCl, 1.5mM MgCl2, .2mM EDTA, 25% glycerol, protease inhibitors) and incubated on ice for 10 minutes. Cells were then spun, the liquid extract removed, and stored at -80˚C.

Western Blot Pax5: 5 µg of protein was mixed with 2x protein loading dye and loaded on a 10% acrylamide gel and electrophoresed in running buffer (125mM Tris-glycine, 0.5% SDS). The protein was transferred to nitrocellulose with electroblotting buffer (25mM Tris, 192mM glycine, 10% MeOH [pH 8.3]). The blot was blocked in 5% donkey serum, 0.1% Tween 20 in 1x PBS, then incubated in anti-Pax5 (1:100) for 2 hours. The blot was then washed in PBS + 0.1% Tween 20 then incubated in donkey-anti-goat-HRP (1:10,000) for 1 hour. The blot was washed then incubated in detector solution (Promega) for 5 minutes and detected using the BioRad documenter.

Western Blot CD19 and CD79a: 10 μg of protein was mixed with equal volume 2x protein loading dye and loaded on a 10% acrylamide gel and electrophoresed in running buffer (125mM Tris-glycine, 0.5% SDS). The protein was transferred to nitrocellulose with electroblotting buffer (25mM Tris, 192mM glycine, 10% MeOH [pH 8.3]). The blot was then blocked in 5% milk, 0.1% Tween 20 in 1x PBS, then incubated in anti-CD19 or anti-CD79a (Santa Cruz) at a dilution (1:500) overnight. The blot was then washed in PBS + 0.1% Tween 20 then incubated in donkey-anti-rabbit-HRP (1:10,000) for 1 hour. The blot was washed then incubated in detector solution (Promega) for 5 minutes. The BioRad gel documentation system was used to image the chemilumeniscence.

Western Blot H3K9: Whole nuclear extracts were mixed with an equal volume of 2x protein loading dye and loaded on a 12% acrylamide gel. The running and transfer of the protein followed the same procedure as the western blot for CD19 and CD79a, only differing in the primary anti-body used which was anti-methyl H3 (Abcam) at a dilution of (1:500).

Western Blot Antibody Removal and Standardization with Actin: Membranes were submerged in stripping buffer (100mM 2-Mercaptoethanol, 2% SDS, 62.5 mM Tris-HCl) and incubated at 50˚C for 30 minutes. Membranes were then washed twice with PBS-T at room temperature and blocked with blocking buffer (5% milk, 0.1% Tween 20 in 1x PBS). Membranes were then incubated in anti-actin (Santa Cruz) at a dilution

(1:250) overnight. The blot was then washed in PBS + 0.1% Tween 20 then incubated in donkey-anti-rabbit-HRP (1:10,000) for 1 hour. The blot was washed then incubated in detector solution (Promega) for 5 minutes. The BioRad gel documentation system was used to image the chemilumeniscence.

Data Analysis: Immunocytochemistry was analyzed by taking pictures of stained cells using the Olympus Fluoview FV500/IX81 confocal microscope. These pictures were quantified based on the intensity of staining using Fluoview review software. Western blot and SDS-gels were analyzed using a BioRad imager with accompanying Quantity1 software. Data was statistically analyzed using the student t-test.

CHAPTER III

RESULTS

Determination of the status of Pax5 expression levels in B cells before, during and after EBV infection:

Since it has been established that the expression of EBV genes in infected cells can alter cellular events including transcription and protein expression, I examined the expression levels of Pax5 protein in B cells throughout EBV lytic replication. It has already been shown that the EBV immediate-early protein BZLF1 can stabilize certain cellular proteins (Adamson et al 2000; Adamson and Kenney 2001; Adamson et al. 2005). Also, preliminary results have demonstrated that Pax5 protein accumulates in BZLF1-expressing cells (Adamson et al, 2005). So I wanted to test whether BZLF1 altered the stabilization of Pax5.

a). Pax5 protein expression levels determined by confocal microscopy:

To examine the Pax5/BZLF1 interaction I performed a time-course study in B cells to monitor Pax5 protein levels during EBV lytic replication. To accomplish this I infected Raji B cells with the EBfaV-GFP virus. Raji B cells were chosen for this specific aim as they express high levels of CD21, the EBV receptor, and can thus be efficiently infected with the EBV virus while also naturally producing the Pax5 protein.

The virus EBfaV-GFP was chosen as it is a green fluorescent protein-marked EBV virus, allowing for easy identification of infected cells through confocal microscopy. Cells were infected with the virus and collected at varying times. Collection times being roughly 0 (uninfected), 24, 41, 65, 73, and 90 hours post-infection.

Cells were prepared through immunocytochemistry with an anti-Pax5 antibody. Cells were then examined with a confocal microscope, and images of cells showing infection (expression of the GFP) were taken (Figure 2). These cells were then quantified using Fluoview confocal software to measure the levels of Pax5 protein in EBV infected cells at varying points of infection (Figure 4).

As seen in Figure 2, by examining without quantification, Pax5 expression levels increased as infection time increased. At 0 hours infection the levels of Pax5 represented were low (Figure 2 panel 1). In contrast, a cell experiencing prolonged infection, such as 73 hours post-infection, Pax5 levels expressed were higher (Figure 2 panel 5).

Each time point of infection was analyzed separately. Cells found to be expressing GFP were circled and quantified for Pax5 expression, as these cells were EBV infected. As seen in Figure 3, GFP expression was minimal at 0 hours of infection as these are uninfected with the EBV virus. EBV gene expression in 24, 41, 65, 73, and 90 hours post-infection were higher than 0 hours infection. This indicated that these cells were indeed infected and the EBV lytic protein BZLF1 was present.

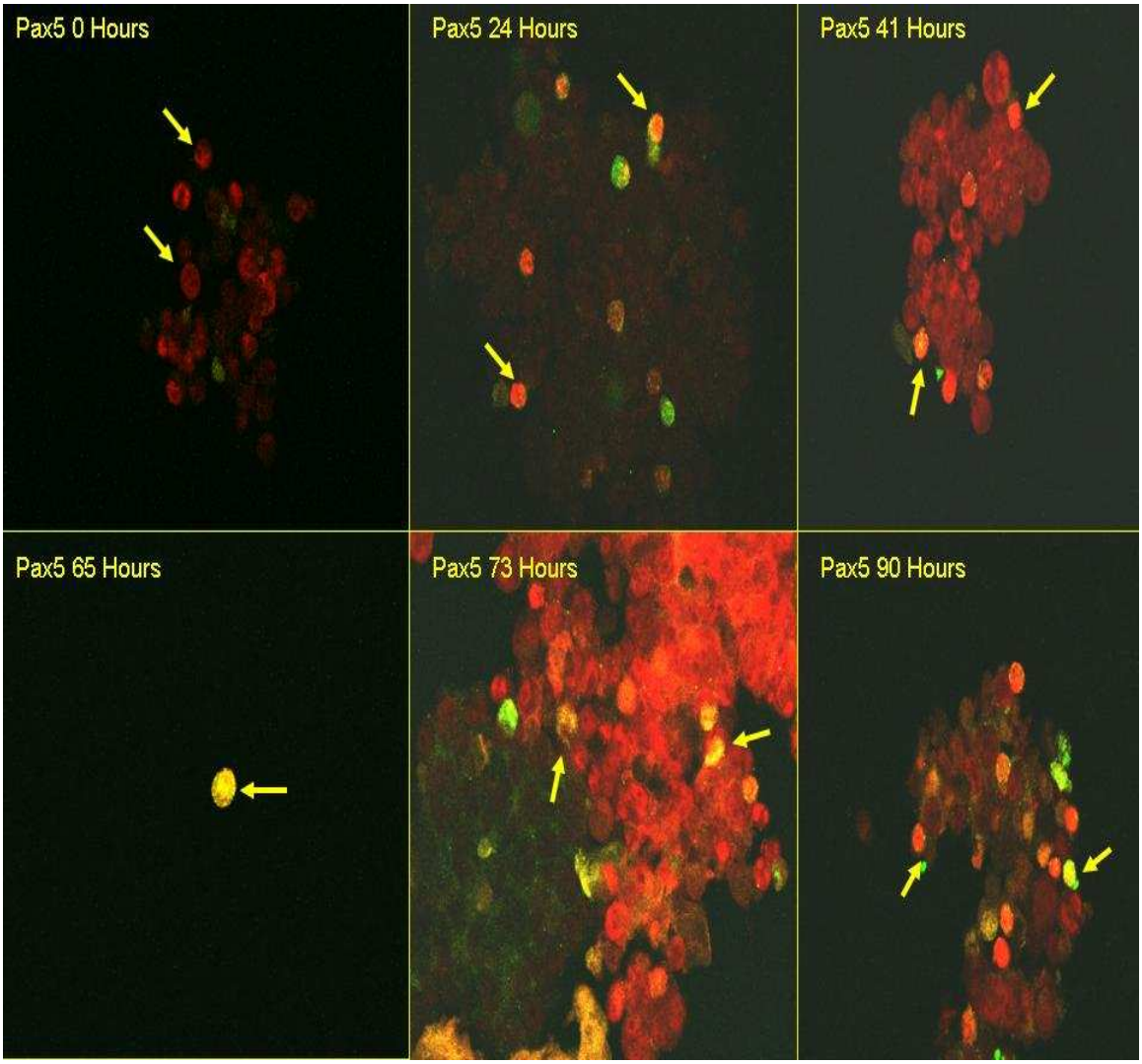

Figure 2: Pax5 protein levels in Raji cells infected with EBfaV-GFP virus at varying time points 0, 24, 41, 65, 73, and 90 hours. Arrows point at specific GFP expressing cells (green fluorescence) showing cells infected by EBV and therefore expressing BZLF1. Pax5 expression is represented by Cy3 staining (red fluorescence).

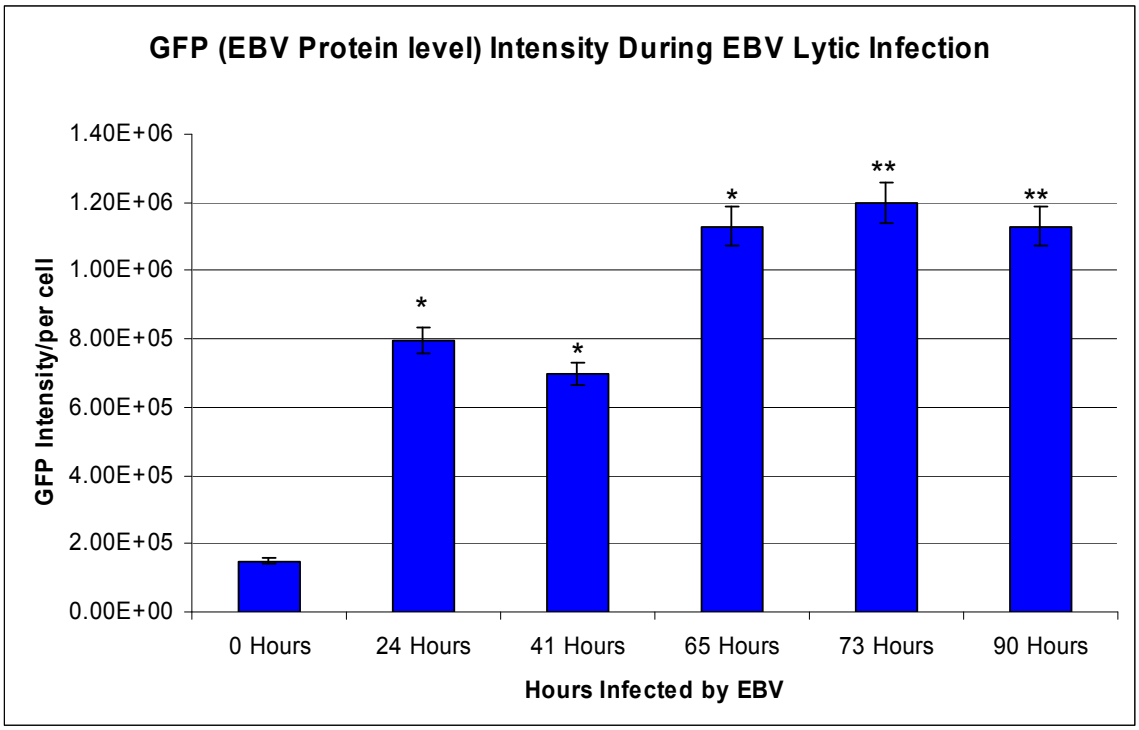

Figure 3: Graph depicting GFP cell staining intensity during different hours of EBV infection. 0 hours (n=42) has the lowest levels of GFP intensity as this represents uninfected cells. 24 (n=29), 41 (n=30), 65 (n=10), 73 (n=42), and 90 (n=42) hours all have relatively the same levels of GFP expression, and are all significantly higher than 0 hours. (* $p<.05$) (** $p<.0005$)

To quantify levels of Pax5 protein, each cell expressing GFP was quantified for Pax5 expression. The more intense the Cy3 expression, the more Pax5 was present. Each indicated time point post-infection had approximately 30 individual cells expressing GFP quantitated and then averaged together. The results shown in Figure 4 indicate that as the level of infection time increased, the level of Pax5 protein also increased before eventually leveling out.

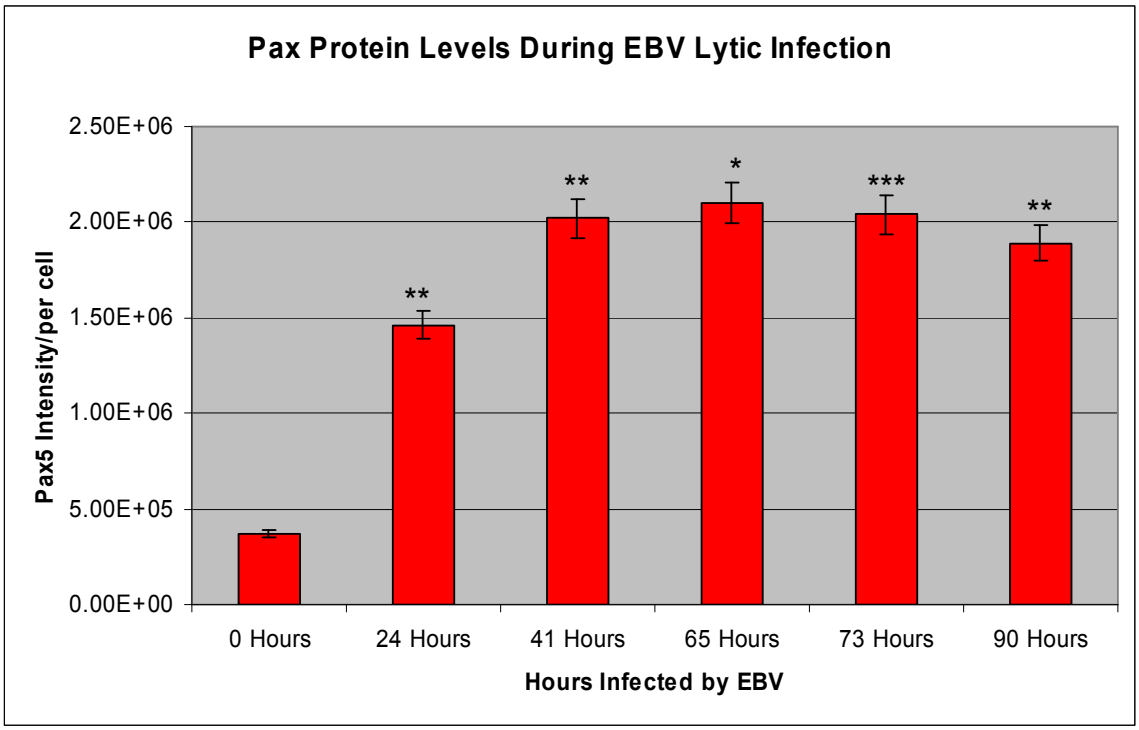

Figure 4: Pax5 protein levels increase as the hours of infection with EBV increase. 0 hours (n=42) indicate cells uninfected with EBV and correspond with the lowest levels of Pax5 protein. 24 hours (n=29) post-infection Pax5 protein levels have increased significantly and eventually plateau by 41 hours (n=30) at 5.5 times their normal level. This trend of increased Pax5 levels continues through 65 (n=10), 73 (n=42), and 90 (n=42) hours post-infection.
(* p<.05) (** p<.0005) (*** p<.000000000005)

As seen in Figure 4, Pax5 levels are normally quite low in Raji cells. The Pax5 levels represented by staining intensity were only 370,000 intensity units when uninfected with EBV. However, this staining intensity number jumped to 1,460,000 intensity units after only 24 hours of infection by EBV. The staining intensity number peaked at 2,100,000 intensity units 65 hours post-infection. This jump in staining intensity between uninfected cells and cells 65 hours post-infection indicated Pax5 levels were altered by EBV lytic replication. Pax5 levels, as seen in Figure 4, reached a point

that is 5.5 the level in uninfected (0 hour) cells. Such an increase in Pax5 protein expression levels could indicate that changes in Pax5 levels during lytic replication play a role in altering the cellular state.

The data in Figure 4, also shows that after 65 hours of infection the Pax5 protein levels began to decline slightly. This small decline is most likely attributed to overall cell death that occurred when cells have been infected upwards of 90 hours. It is likely that once EBV lytic infection is established Pax5 levels will remain at a constant and increased level.

b). Pax5 protein expression levels determined by western blot analysis:

To complement the immunocytochemistry, I performed Western blot analysis to examine overall cellular levels of Pax5 protein. For this I collected/extracted protein from the same time points listed, 0, 24, 41, 65, 73, and 90 hours. Equal amounts of protein were run on an SDS-PAGE gel. The proteins were transferred to nitrocellulose and immunoblot analysis was performed with an anti-Pax5 antibody (Figure 5). The protein bands from the varying time points were quantified with ChemicDoc software (Figure 6).

As seen in Figure 5, the results from performing a western blot correlated with the results gathered from confocal microscopy. The level of Pax5 protein was less in uninfected cells than those that were infected by EBV and as infection time increased the level of Pax5 protein also increased, while finally peaking around 65 hours post-infection (Figure 5).

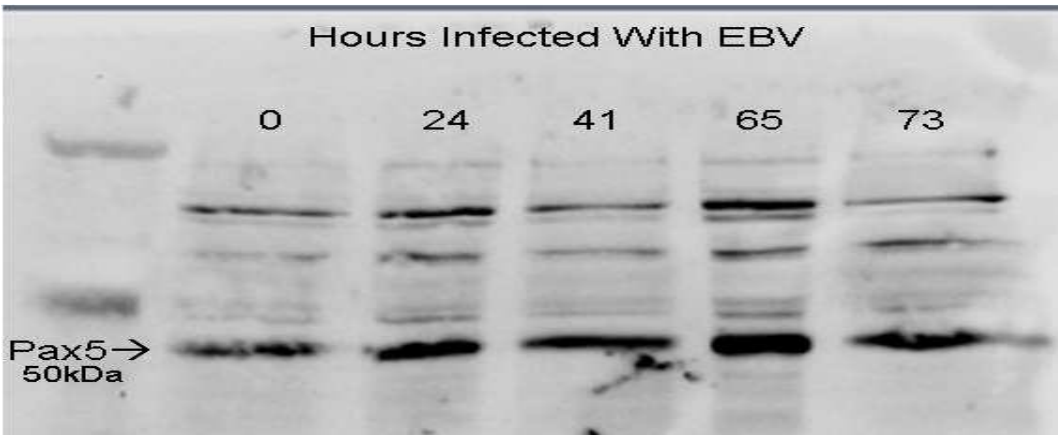

Figure 5: Western blot of Pax5 protein levels at varying points of EBV lytic infection. 0 hours represents protein levels from uninfected cells. The other 4 time points represent hours post-infection. Pax5 is found at 50kDa. Protein levels were standardized using tubulin protein levels.

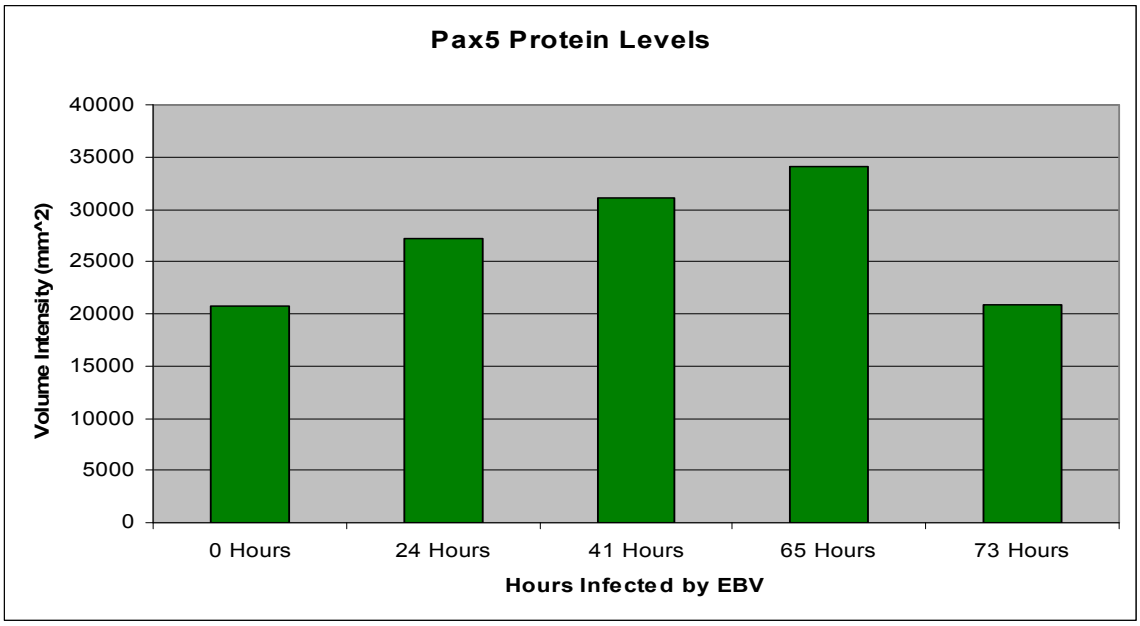

Figure 6: Pax5 protein levels increased as time infected with EBV increased determined by western blot analysis. Quantification of Pax5 western blot showing that Pax5 protein levels at 0 hours are significantly less than Pax5 protein levels in EBV infected cells. Pax5 protein levels continue to increase up to 65 hours post-infection before cell death drops Pax5 levels. All protein bands were standardized using tubulin protein to ensure equal loading.

Pax5 protein levels at 0 hours infection were significantly less than cells that were infected by EBV. At only 24 hours post-infection cells infected with EBV had more Pax5 protein present. For this data there was approximately 1.4 times Pax5 protein in cells infected for 24 hours by EBV in comparison to uninfected cells. The Pax5 levels slightly increased 65 hour post-infection to approximately 1.65 times the level in uninfected cells (Figure 6)

At 73 hours, the Pax5 protein levels decreased relative to hour 65, and were identical to uninfected cells. Decrease in Pax5 levels could be explained by cell death. The stress on cells infected by EBV for such a long period may accelerate cellular death resulting in an inability to accurately determine protein levels past 65 hours. This idea is supported when looking at cells infected with EBV for any prolonged period of time under a microscope. Many cells appear shriveled or dead in comparison to uninfected cells. For this reason it was difficult to collect and analyze cells for Pax5 protein at 90 hours post-infection, due to such a high rate of cell death that had occurred. Overall, B cells infected with the lytic replicating Epstein-Barr virus experienced an increase in Pax5 protein. The BZLF1/Pax5 complex resulted in Pax5 levels increasing to at least 1.65 times their normal levels during lytic infection.

c). Pax5 transcription levels in cells expressing BZLF1

To determine whether this increase in Pax5 levels during EBV lytic infection was caused by an increase in Pax5 mRNA or by stabilization of the Pax5 protein by BZLF1 I performed a time course RT-PCR study. Raji cells were infected with the EBV virus and collected at times, 0, 24, 41, 65, 73, and 90 hours. RNA from each post-infection time was extracted and RT-PCR performed using Pax5 specific primers. The RT-PCR products were run on an agarose gel (Figure 7) and the bands quantified using BioRad quantification software (Figure 8).

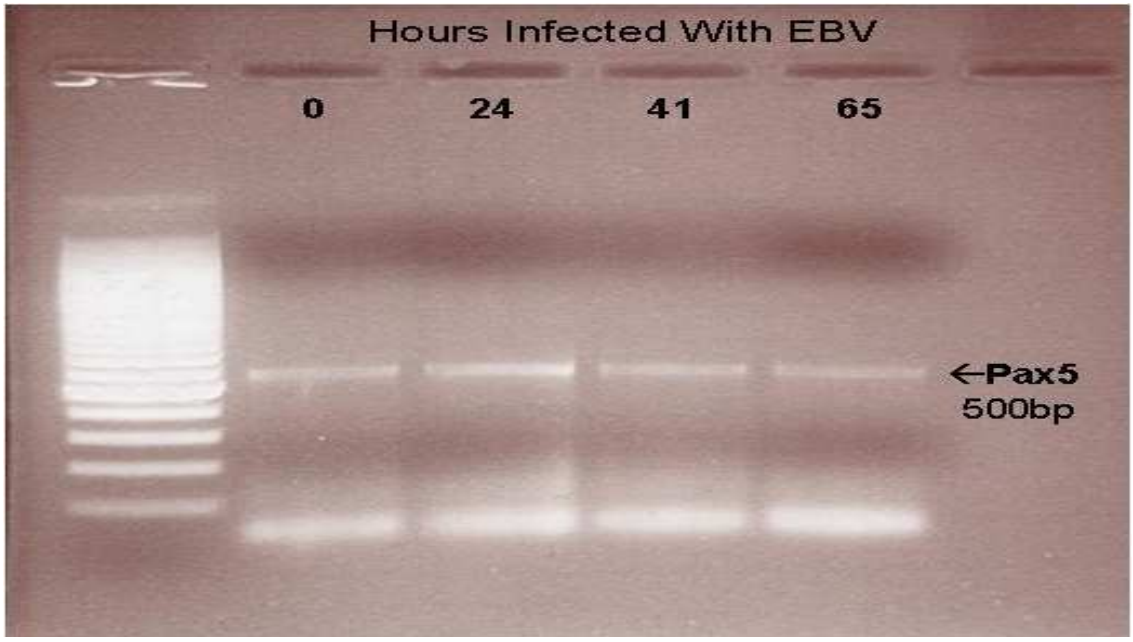

Figure 7: Gel showing that RT-PCR Pax5 products are identical regardless of hours infected by EBV. 0 hours represent EBV uninfected cells, the other time points represent hours post-infection. Pax5 products are found at 500bp

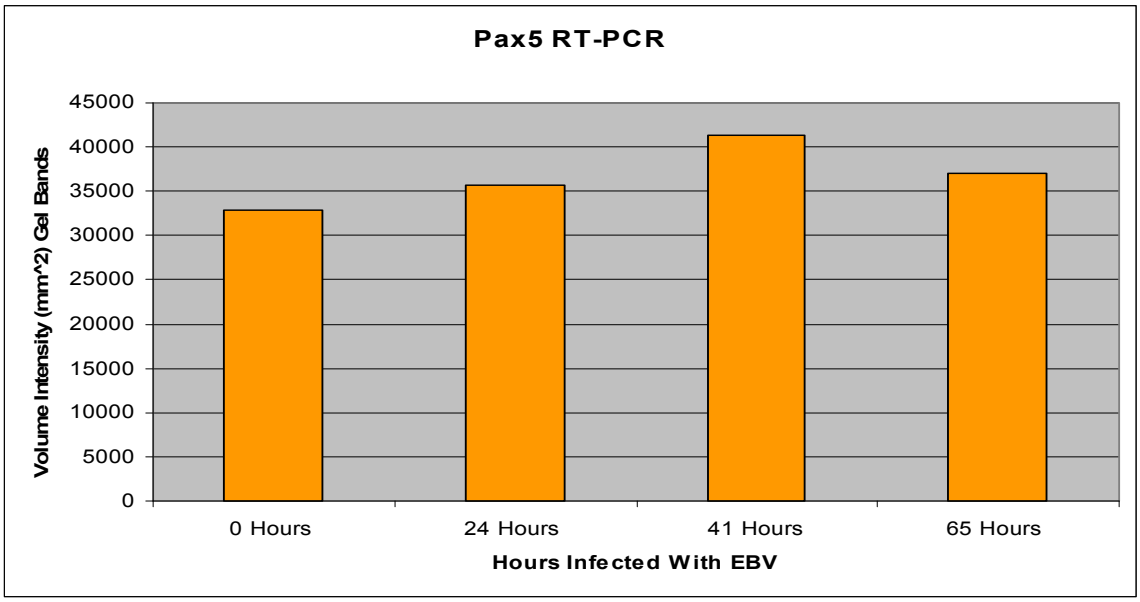

Figure 8: Quantification of Pax5 RT-PCR products showing that RT-PCR products remain constant regardless of EBV infection. Each time point represents hours infected by EBV.

As seen in Figure 7, it appears as if there is no overall change in Pax5 mRNA levels as infection time increases. The bands corresponding to Pax5 RT-PCR products for each of the time points listed visually appeared to be identical within the gel. The bands were quantified for total Pax5 mRNA products by looking at overall volume intensity (Figure 8). By quantifying the bands it is clear that there is no significant change in Pax5 mRNA levels when cells were infected with EBV. The RT-PCR products remained constant at all time points. If transcriptional activity was affected by EBV and this accounted for the increase in Pax5 present, there should be an increase in Pax5 RT-PCR products that corresponded to the increase in Pax5 protein levels. This is not the case,

which is demonstrated by Figure 8, where at 65 hours post-infection the mRNA levels were the same as those seen at 0 hours.

It appears that an increase in Pax5 mRNA levels is not causing the increase in Pax5 protein seen during lytic infection. BZLF1 has been known to stabilize other proteins. So it is plausible that BZLF1 may act to stabilize the protein Pax5. Overall, I was able to establish two possible trends during EBV lytic infection. First, Pax5 protein levels increased during EBV lytic infection. Second, the increase in Pax5 protein levels most likely is not caused by an increase in Pax5 transcription. Instead, this increase is likely caused by a stabilization of Pax5 protein through its physical interaction with BZLF1. These results are important to investigate further as changes in Pax5 levels may cause many different changes to cellular activity.

Examination of the histone methylation state of chromatin in BZLF1-expressing cells:

BZLF1 tethers Pax5 protein to mitotic chromosomes, and is capable of demethylating histone H3 (Johnson et al. 2004). BZLF1 is involved in EBV lytic gene control, and has also been linked to other methylation events (Bhende et al. 2004). Methylation act as marks for chromatin, and changing these marks alters many aspects of chromatin, including compaction, transcription, and access to recombination machinery. Any change in methylation may then have serious long-term consequences for infected cells, as alterations in transcription and recombination can potentially set the stage for the development of cancer. To determine whether the increase in Pax5 as a result of BZLF1

results in any alteration to global methylation I examined if there were any changes in global methylation of histone-H3 lysine-9.

a). H3K9 methylation levels in D98/HE-R1 transfected cells as determined by confocal microscopy:

To examine the methylation state of cells, I used confocal microscopy to quantify the levels of methylated lysine-9 of histone-H3 in EBV-positive D98/HE-R1 cells. EBV-positive D98/HE-R1 cells were used as they can be transfected with both a BZLF1 expression vector as well as a Pax5 expression vector. This allowed me to compare the experimental condition of BZLF1 and Pax5 co-expression with three control conditions: 1. Pax5 expression alone; 2. BZLF1 expression alone; and 3. Empty control vector. D98/HE-R1 cells were transfected with all four conditions for 48 hours and post-transfection immunostained with both anti-BZLF1 and anti-methylated histone H3K9 antibodies.

After immunostaining I imaged mitotic chromosomes of all four conditions (Figure 9). Since BZLF1 has been shown to tether Pax5 to mitotic chromosomes, I focused my studies specifically to mitotic cells. Cells were grouped into two categories, those expressing BZLF1 (BZLF1 alone and BZLF1+Pax5 condition) and those not expressing BZLF1 (Pax5 alone and control vector). Within each group, the anti-methylated histone H3K9 antibody staining and the DNA staining was quantified for each set of mitotic chromosomes. From this data I then calculated the ratio of methylated histone H3 intensity to the DNA staining intensity (Figure 10). By comparing the ratios

between the four conditions, I determined the effect that the BZLF1/Pax5 complex had on methylation status of H3K9.

Only mitotic cells were quantified, as indicated by the yellow arrows in Figure 9. The easiest mitotic stage to identify was metaphase, and this resulted in many of the cells quantified being in this cell state. It is difficult to measure changes in H3K9 methylation because H3K9 methylation is a global cellular event, and because H3K9 methylation levels will be directly proportional to overall cellular DNA. To control for this variable, DNA was also quantified and a ratio of global H3K9 methylation to global DNA levels was determined.

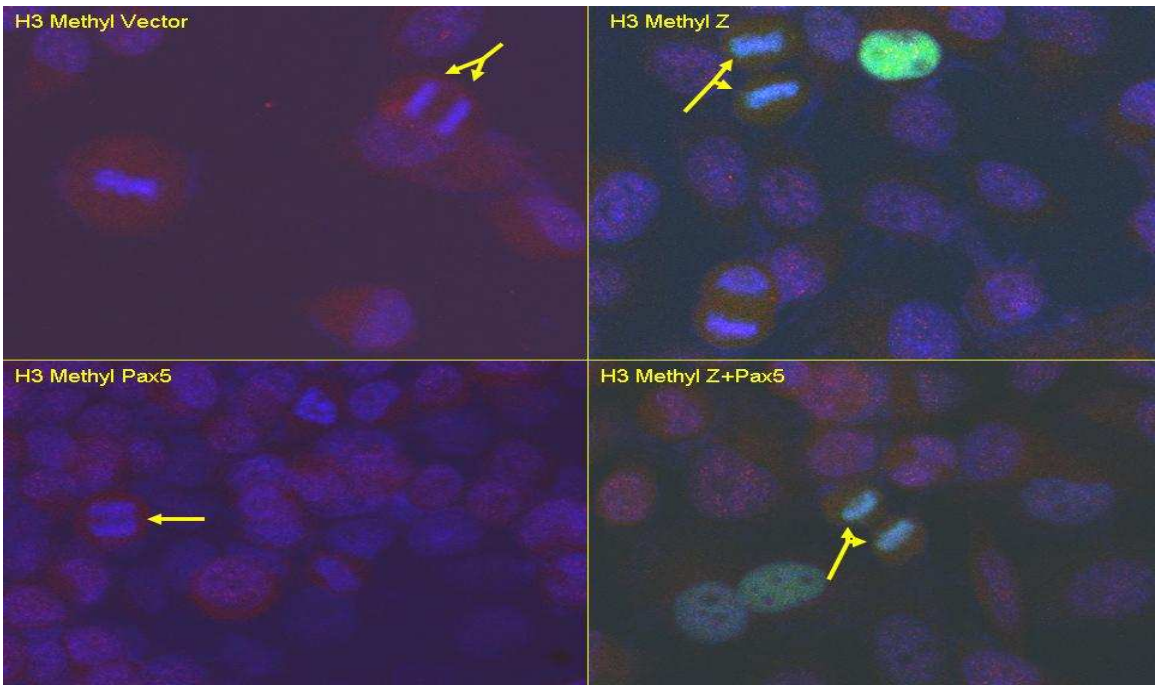

Figure 9: Confocal images of D98/HE-R1 transfected cells stained for H3K9 methylation (red), BZLF1 expression (green) and DNA (blue). Arrows point to mitotic cells, indicating these cells were quantified. All four conditions are represented. Cells not expressing BZLF1 on the left, Vector control and Pax5 alone. Cells expressing BZLF1 on the right, Z alone and Z+Pax5.

Figure 10 shows that when BZLF1 was being expressed in the presence of Pax5 there was an increase in the overall global methylation levels of H3K9. Using the vector as a base control, there was a slight increase in H3K9 methylation levels when only BZLF1 was present but not of any significance. There was then a mild decrease in H3K9 methylation levels when only Pax5 was present but not of any significance. Finally when BZLF1 and Pax5 were expressed together there was a significant increase in global H3K9 methylation levels.

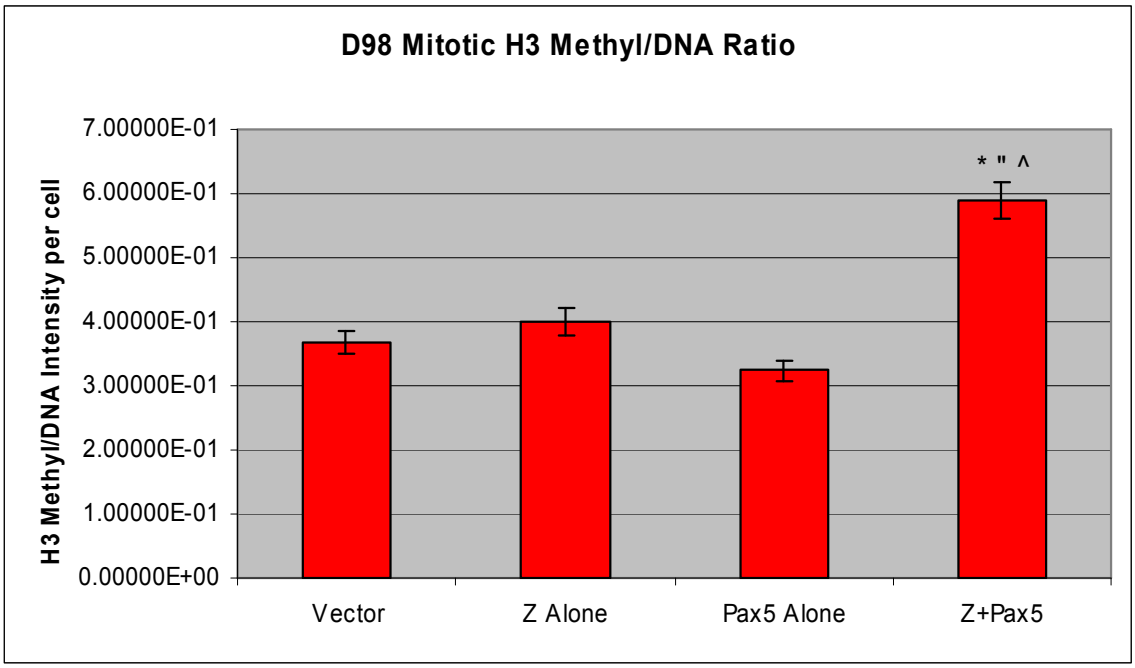

Figure 10: Quantification of D98/HE-R1 mitotic chromosomes for H3K9 methylation controlled for by ratio to overall DNA levels .H3K9 methylation levels increase almost 2 fold when BZLF1 and Pax5 are expressed together. Each bar represents a different condition 1. Vector (n=22) 2. BZLF1 alone (n=28) 3. Pax5 alone (n=21) 4. Z and Pax5 (n=28)
Student t-Test performed to indicate level of significance from *-vector, "-Z alone, ^- Pax5 alone ($p<.05$)

Figure 10 matches the hypothesized outcome for the first three conditions. BZLF1 alone is known to have histone methylation activity and here there was a slight increase in H3K9 methylation levels. Pax5 alone is known to be a histone demethylase and there was a slight decrease in H3K9 methylation levels. However, the results for BZLF1 and Pax5 together were unexpected. The BZLF1/Pax5 complex lead to an increase in overall global H3K9 methylation levels. The most important comparison to make is between BZLF1/Pax5 and Pax5 alone. As the condition Pax5 alone would represent a normal B cell state and BZLF1/Pax5 would represent an EBV infected B cell state. When comparing these two conditions there was a 2 fold increase in overall H3K9 methylation levels when BZLF1 and Pax5 were both present.

I also determined the H3K9 global methylation levels in D98/HE-R1 non-mitotic cells by quantifying cells that were not in a mitotic cell state (data not shown). The results of this analysis were similar to those found when looking at mitotic D98/HE-R1 cells. There was once again a 2 fold increase in overall H3K9 methylation levels in BZLF1/Pax5 cells in comparison to Pax5 alone cells. This result suggested that although BZLF1 is known to tether Pax5 to mitotic chromosomes, the consequences of this action resonate throughout the entire cell cycle where increased H3K9 methylation levels remain

b). H3K9 methylation levels in EBV-positive Raji B cells determined by confocal microscopy:

To further examine the effect of the BZLF1/Pax5 complex on the methylation status of histone H3 I examined EBV-positive B cells for H3K9 methylation.
I transfected Raji cells with a BZLF1 expression vector or a control vector. Only two conditions (Pax5 alone and BZLF1+ Pax5) were examined as Raji cells are B cells that naturally produce Pax5. After 48 hours post-transfection, I immunostained the cells with the anti-BZLF1 and anti-methylated histone H3K9 antibodies (Figure 11). I then performed the same quantitation methods as with the D98/HE-R1 cells. The ratio of methylated histone H3 intensity to the DNA staining was calculated and a comparison between the two conditions made (Figure 14).

As seen in Figure 11, mitotic cells were stained for methylated H3K9, as indicated by the yellow arrows. Mitotic Raji cells were quite small and it was difficult to determine their cell state. In Figure 11 it is clear that unlike D98 cells where mostly the metaphase state was quantified, Raji cells were quantified using a variety of mitotic stages, such as prophase, Figure 11 panel one, and metaphase, Figure 11 panel 2. For the first condition only cells found in a mitotic state were quantified. For the second condition, BZLF1 and Pax5, only cells expressing BZLF1 and in mitosis were quantified. BZLF1 expression was determined by the presence of green fluorescence

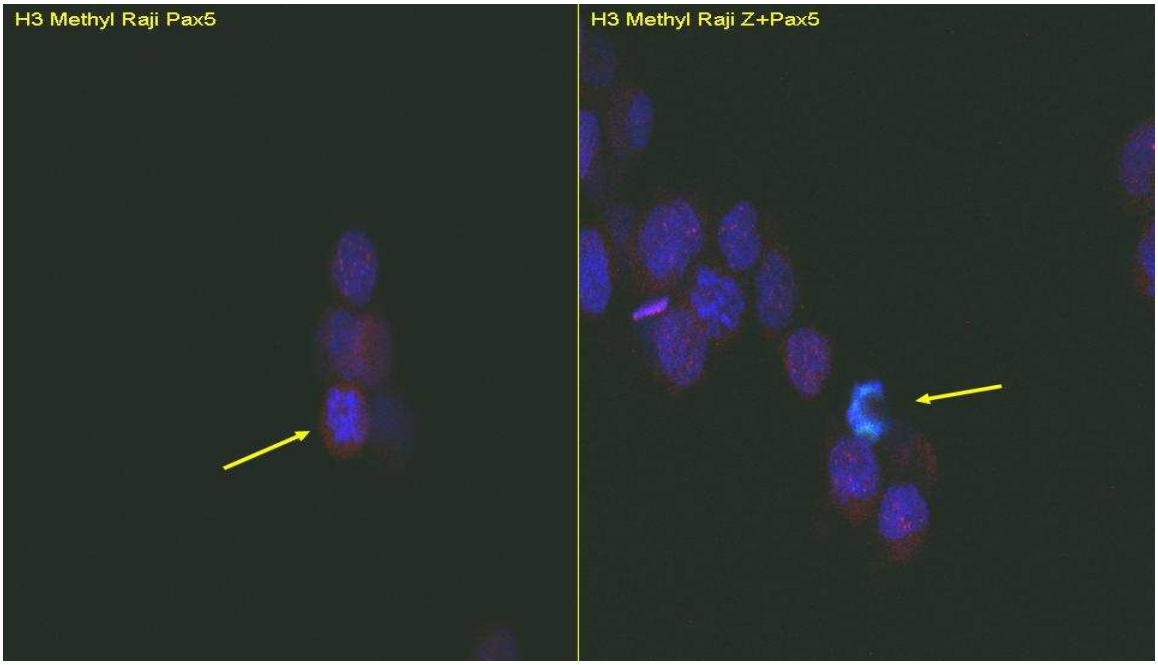

Figure 11: Confocal images of Raji transfected cells stained for H3K9 methylation (red), BZLF1 expression (green) and DNA (blue). Arrows point to mitotic cells, indicating these cells were quantified. Two conditions are represented. Cells transfected with a control vector on the left. Cells transfected with a BZLF1 expression vector on the right.

H3K9 methylation levels were quantified for both transfection conditions (Figure 12). While looking at overall H3K9 methylation levels there appeared to be a slight increase in H3K9 methylation levels in Raji cells transfected with a BZLF1 expression vector in comparison to cells transfected with only a control vector. These data were controlled by taking the ratio of H3K9 methylation (Figure 12) to the overall amount of DNA present (Figure 13). The overall amount of DNA per cell in each quantified cell was essentially identical between the control cells and BZLF1 transfected cells.

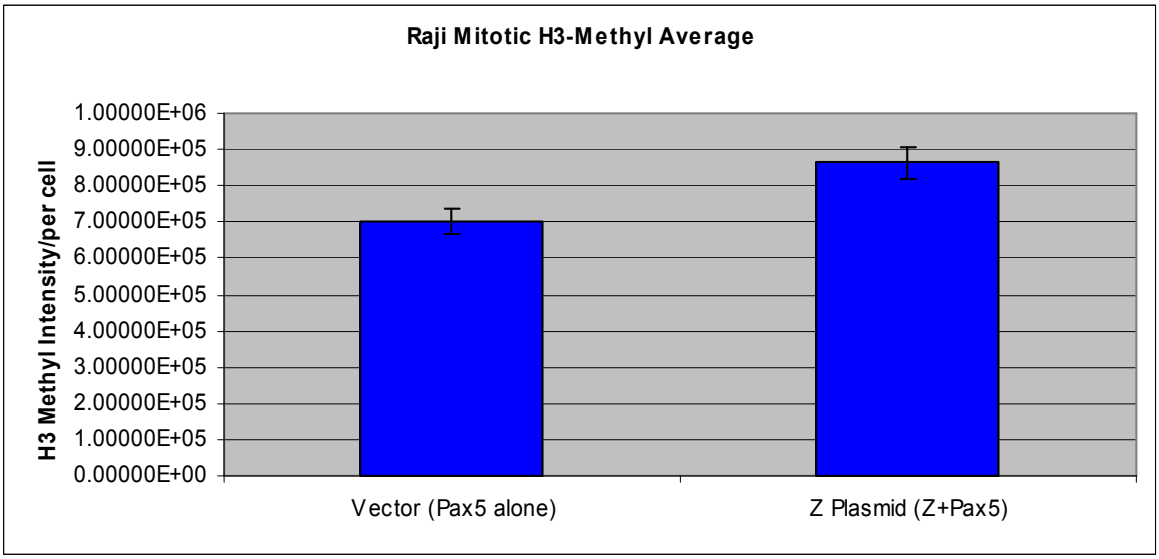

Figure 12: Mitotic Raji cell average H3K9 global methylation levels are slightly increased in cells transfected with a BZLF1 expression vector. Results are averages of at least 25 separate cells.

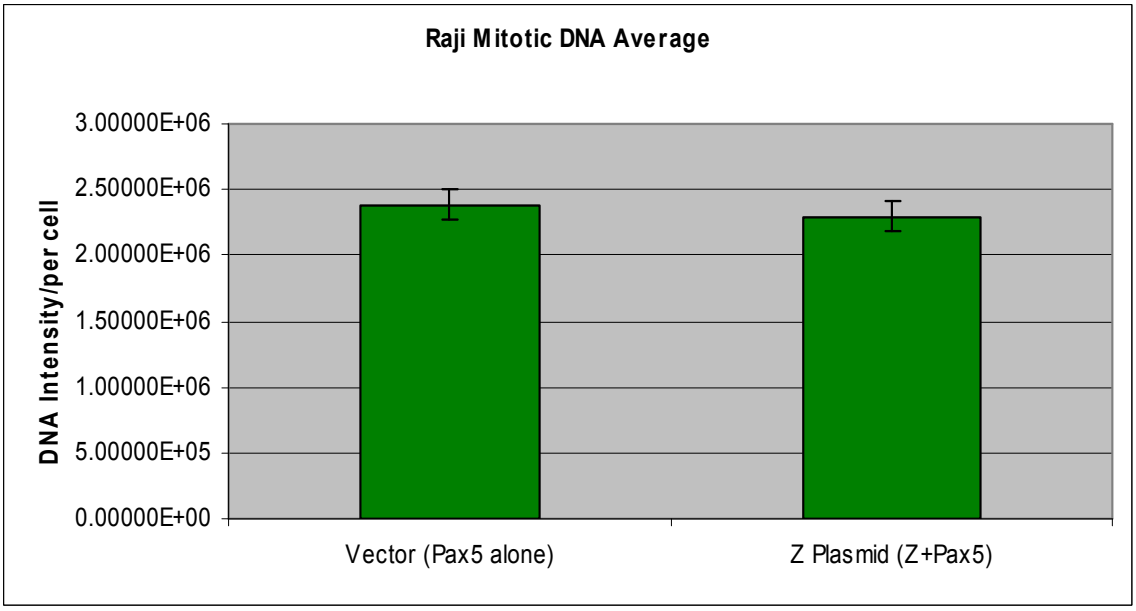

Figure 13: Mitotic Raji cell average global DNA levels are nearly identical for both vector transfected and BZLF1 expression transfected cells. Results are averages of at least 25 separate cells.

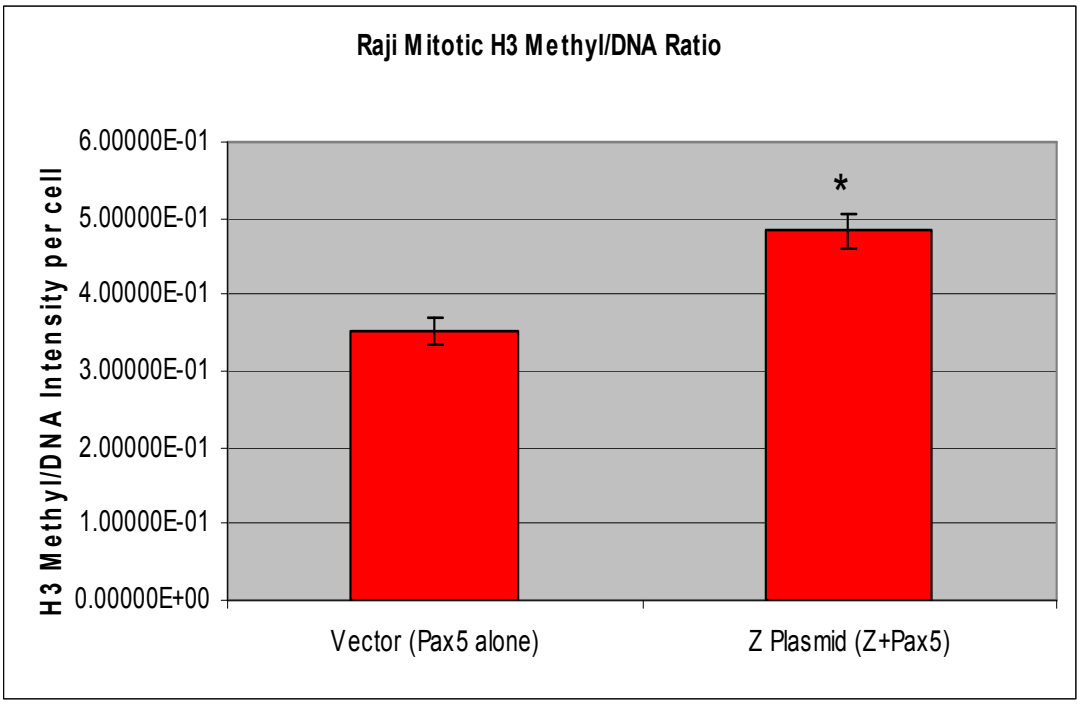

Figure 14: Quantification of transfected Raji cell mitotic chromosomes for H3K9 methylation was controlled for by ratio to overall DNA levels. H3K9 methylation levels increase 1.4 fold when BZLF1 and Pax5 are expressed together. Condition one, a control expression vector (n=28), represents Pax5 alone. Condition two, a BZLF1 expression vector (n=20), represents Pax5 in the presence of BZLF1. (* $p<.05$)

The results are similar to those found when D98/HE-R1 cells were transfected. Raji cells expressing both Pax5 and BZLF1 have increased levels of global H3K9 methylation, 1.4 times the normal levels (Figure 14). These results supported the suggestion that the BZLF1/Pax5 complex results in an increase in global H3K9 methylation levels.

c). H3K9 methylation levels in D98 transfected cells determined by western blot analysis:

To corroborate the immunocytochemistry, I performed Western blot analysis to examine overall cell H3K9 methylation levels. For this I prepared nuclear extracts from D98/HE-R1 transfected cells for each of the four conditions listed before 1. Vector; 2. BZLF1 alone; 3. Pax5 alone; and 4. BZLF1 and Pax5. Equal protein amounts of these nuclear extracts were run on an SDS-PAGE gel. These were then transferred to nitrocellulose, and immunoblot analysis was performed with an anti-H3K9 methylation antibody (Figure 15). The bands from the varying conditions were quantified (Figure 16).

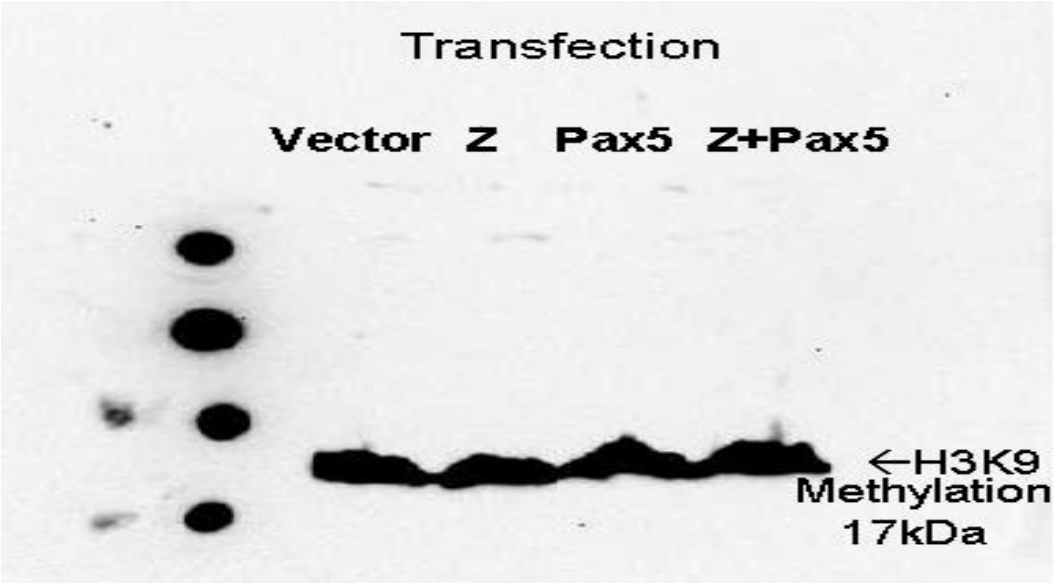

Figure 15: Western Blot of H3K9 methylation levels for varying transfection conditions showing increased H3K9 methylation when BZLF1 and Pax5 are expressed together. The four conditions shown are control vector, BZLF1 vector (Z), Pax5 vector (Pax5), and BZLF1 and Pax5 vectors together (Z+Pax5). The methylated H3K9 band is found at 17kDa

The H3K9 bands shown in Figure 15 were quantified to determine overall volume intensity and therefore overall H3K9 methylation levels. If the bands seen in Figure 15 were to follow the same results as seen in Figure 10 (when immunocytochemistry was performed using the same conditions), then there should be an increase in H3K9 methylation levels when BZLF1 and Pax5 are both being expressed. As shown in Figure 16, there appears to be a slight increase in methylated H3K9 protein in BZLF1 and Pax5 transfected cells. This increase correlated with the confocal data (Figure 9 and 10).

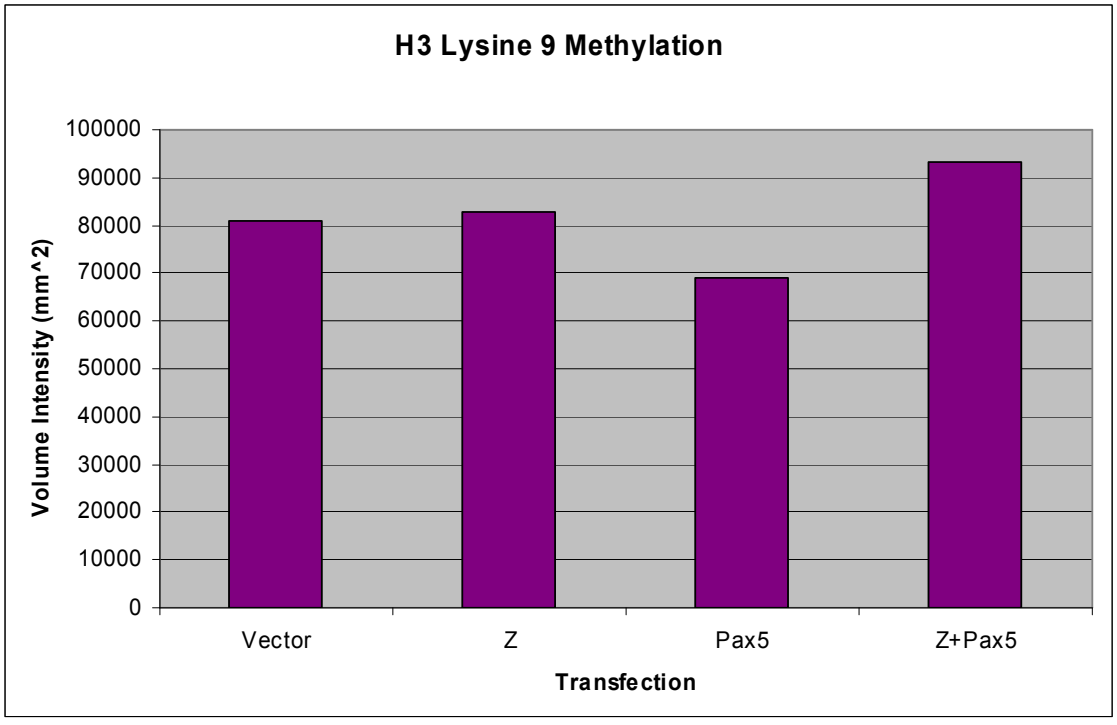

Figure 16: Quantification of D98/HE-R1 extract H3K9 methylation western blot. H3K9 methylation levels increase when BZLF1 and Pax5 are expressed together. Each bar represents a different condition 1. Vector, 2. BZLF1 alone, 3. Pax5 alone, 4. BZLF1 and Pax5.

Using the vector as a base control there was a slight increase in H3K9 methylation levels when BZLF1 is expressed alone. There was also a slight decrease in H3K9 methylation levels when Pax5 is expressed alone. When both BZLF1 and Pax5 were expressed together there appears to be a significant increase in H3K9 methylation levels. Once again the most important comparison to make was between Pax5 expression alone and BZLF1 and Pax5 together. Pax5 alone represented normal EBV uninfected B-cell activity, where as BZLF1 and Pax5 together represented an EBV infected B-cell lytic state. When comparing these two states there was the largest change in H3K9 methylation levels.

Overall I was able to establish a very important and unique trend caused by the increased levels of Pax5 observed in the first aim of this experiment. BZLF1 and Pax5 physically interacted and this interaction leads to the increased levels of Pax5 and the BZLF1/Pax5 complex binding to mitotic chromosomes. The binding of the BZLF1/Pax5 complex, which can act as an epigenetic modifier, resulted in an increase in H3K9 methylation levels. This is an important result as changes in histone methylation levels can result in many different changes within a cell. One very important aspect controlled by histone methylation is the expression or repression of certain tumor suppressor genes.

Examination of the protein expression levels of Pax5 transcriptional targets in BZLF1-expressing and EBV-infected B cells

Pax5 is a transcription factor that transactivates important targets for B cell differentiation, like CD79a and CD19. To determine whether the binding of BZLF1 to Pax5 effects how Pax5 functions I looked at Pax5 targets. Since differentiation determines B-cell fate, any changes in transcriptional activity of specific genes may create significant consequences for the infected cell. The Pax5 targets CD19 and CD79a appear to be altered in B cell leukemias and so it was important to establish whether EBV, specifically BZLF1, leads to altered expression of Pax5 target gene proteins.

a). CD79a protein expression levels determined by confocal microscopy:

To accomplish this aim I quantified the level of CD79a protein in BZLF1 expressing or EBV lytically replicating B cells. I transfected Raji cells with a control or BZLF1 expression plasmid. I also infected Raji B cells with the EBfaV-GFP virus, while also leaving a group of cells uninfected as a control. 48 hours post-transfection or post-infection, cells were stained through immunocytochemistry with an anti-CD79a antibody, as well as an anti-BZLF1 antibody for transfected cells. Cells were then examined by confocal microscopy and images of infected cells (GFP or BZLF1 staining) were taken (Figure 17). Uninfected and control vector transfected cells were also analyzed. These cells were then quantified using Fluoview confocal software to measure the levels of CD79a staining intensity from the four conditions listed (Figure 18).

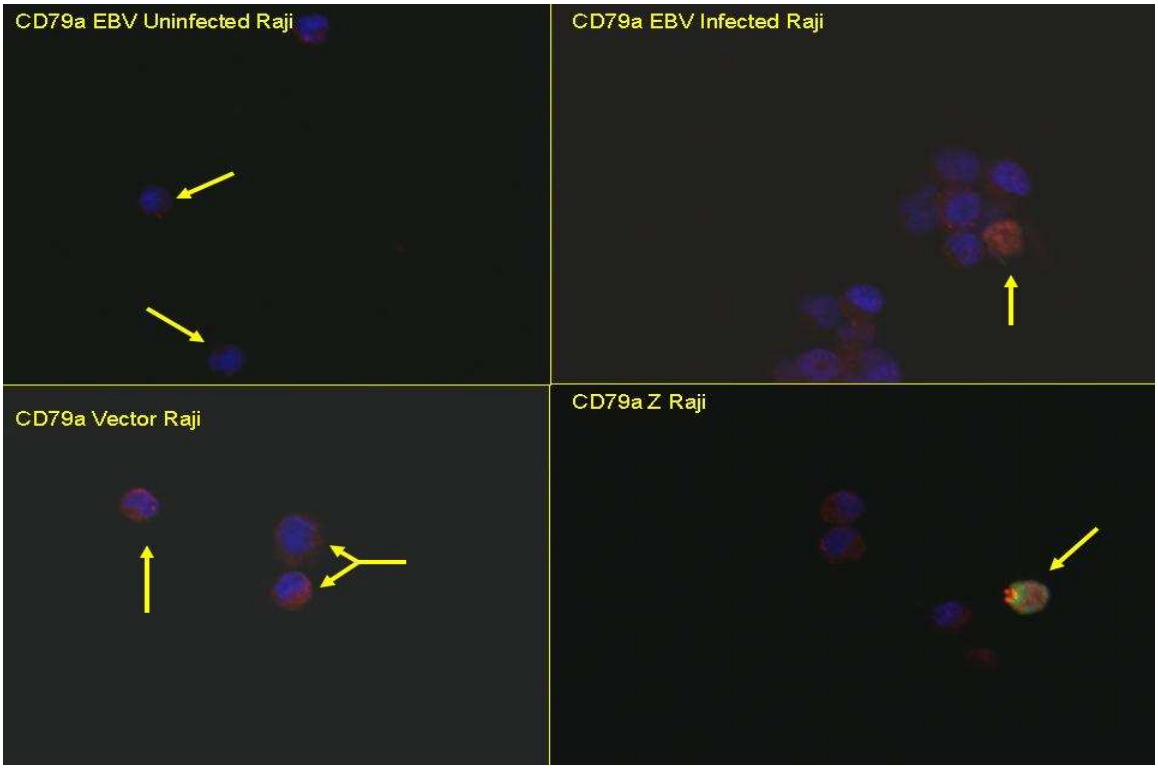

Figure 17: Confocal images of Raji cells stained for CD79a (red), BZLF1/GFP expression (green) and DNA (blue). Arrows point to cells that were quantified. Four conditions are represented. EBV uninfected cells top left, EBV infected cells top right, control vector transfected cells bottom left, BZLF1 transfected cells bottom right.

Figure 17 shows images of all four conditions that were analyzed. The top left panel are stained cells that were uninfected with EBV. These appear to have minimal staining for CD79a. Cells in the top right panel are cells that were infected with EBV. Only cells that were fluorescing green were quantified as these are cells infected with EBV virus. These cells when quantified were compared to the uninfected cells in the top left panel. The bottom left panel includes images of cells transfected with the control expression vector. These cells were quantified and compared to the cells in the bottom

right panel. The bottom right panel contains cells that were transfected with the BZLF1 expression plasmid. Once again only cells fluorescing green fluorescence were quantified as this indicated transfection with the BZLF1 expression plasmid.

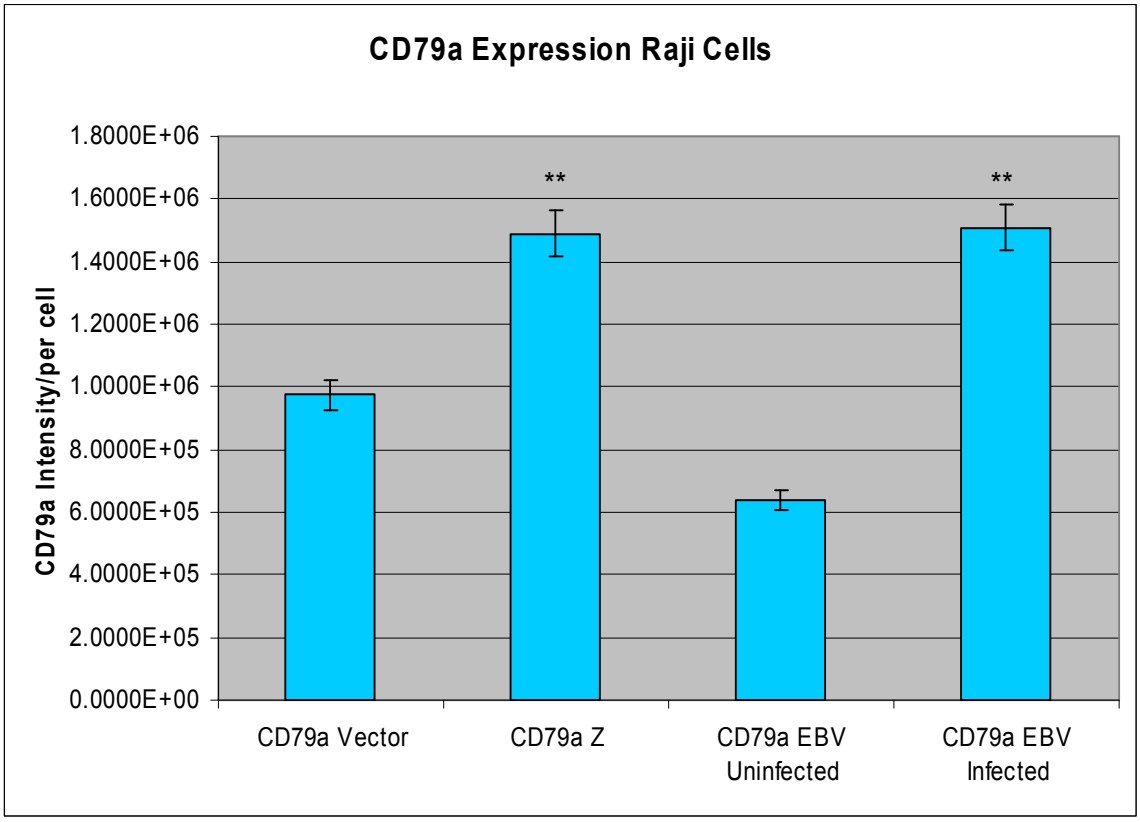

Figure 18: Average quantification of CD79a levels from confocal microscopy. CD79a protein levels significantly increase when infected with EBV or BZLF1 is present. Four conditions shown, vector expression, BZLF1 expression, EBV uninfected, and EBV infected.
** $p<.0005$ (n=40)

Figure 18 shows the quantification of the immunocytochemistry and the imaging represented in Figure 17. Each column depicted is an average of at least 40 different cells. It is clear from the graph that CD79a protein levels increased when BZLF1 was expressed and when cells were infected with EBV. In comparison CD79a EBV infected cells and CD79a EBV uninfected cells, there is a significant increase in CD79a staining in the infected cells of approximately 2.5 fold. To determine if this increase was caused by the EBV lytic protein BZLF1 and its interaction with Pax5, I compared B cells transfected with BZLF1 expression vector to B cells transfected with the control vector. The data indicates that CD79a protein levels are significantly greater in BZLF1 transfected cells (Figure 18). This indicated that the BZLF1 protein, itself, can lead to increased CD79a protein levels. The most likely explanation is that the BZLF1 physical interaction with Pax5, which results in increased levels of Pax5, was responsible for the increased levels of Pax5 target CD79a.

b). CD79a protein expression levels determined by western blot analysis:

CD79a protein levels were also compared by western blot analysis. I isolated proteins from BZLF1-transfected, control transfected, uninfected, and infected Raji cells. Equal amounts of protein extracts were run on an SDS-PAGE gel. These were transferred to nitrocellulose, and immunoblot analysis was performed with an anti-CD79a antibody (Figure 19). The bands were quantified and volume intensities compared (Figure 20).

From the immunoblot, seen in Figure 19, the four different bands were quantified to determine overall volume intensity and therefore overall CD79a levels. The bands

were standardized using actin protein to ensure equal loading of protein. If the bands seen in Figure 19 were to follow the same results as seen in Figure 18 then there should be an increase in CD79a levels when cells are infected with EBV or expressing BZLF1. As seen in Figure 20 this indeed was the case, and the results from the western blot analysis were identical to the results determined from confocal microscopy (Figure 18)

The results in Figure 20 are similar to the results seen in Figure 18, when using immunocytochemistry to determine CD79a protein levels. Comparing protein levels between EBV uninfected cells and EBV infected cells, an increase in CD79a is detected in EBV infected cells (Figure 20).

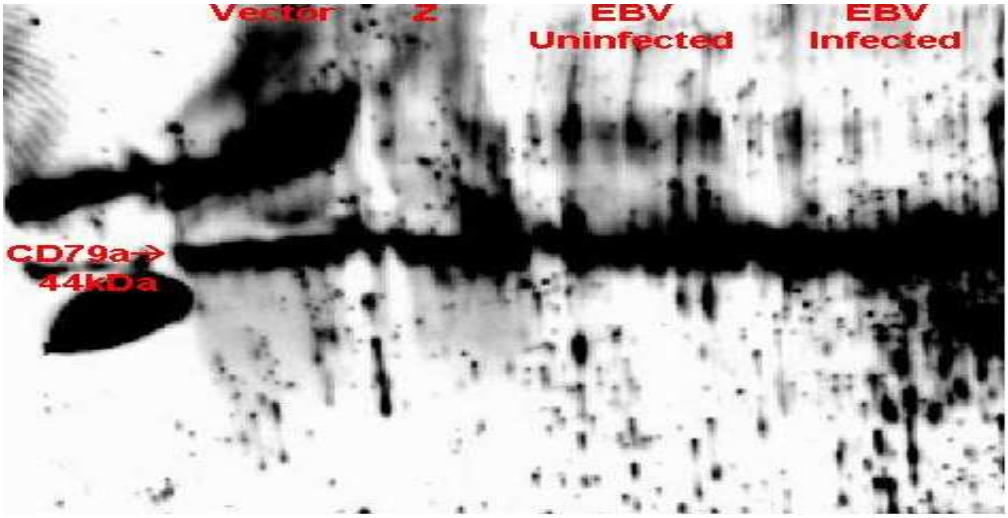

Figure 19: Western Blot of CD79a protein levels for varying transfection conditions showing increased CD79a when EBV infected or BZLF1 is expressed. The four conditions shown from Raji cells are 1) transfected with control vector (vector); 2) transfected with BZLF1 expression vector (Z); 3) EBV uninfected; and 4) EBV infected. CD79a is found at 44kDa.

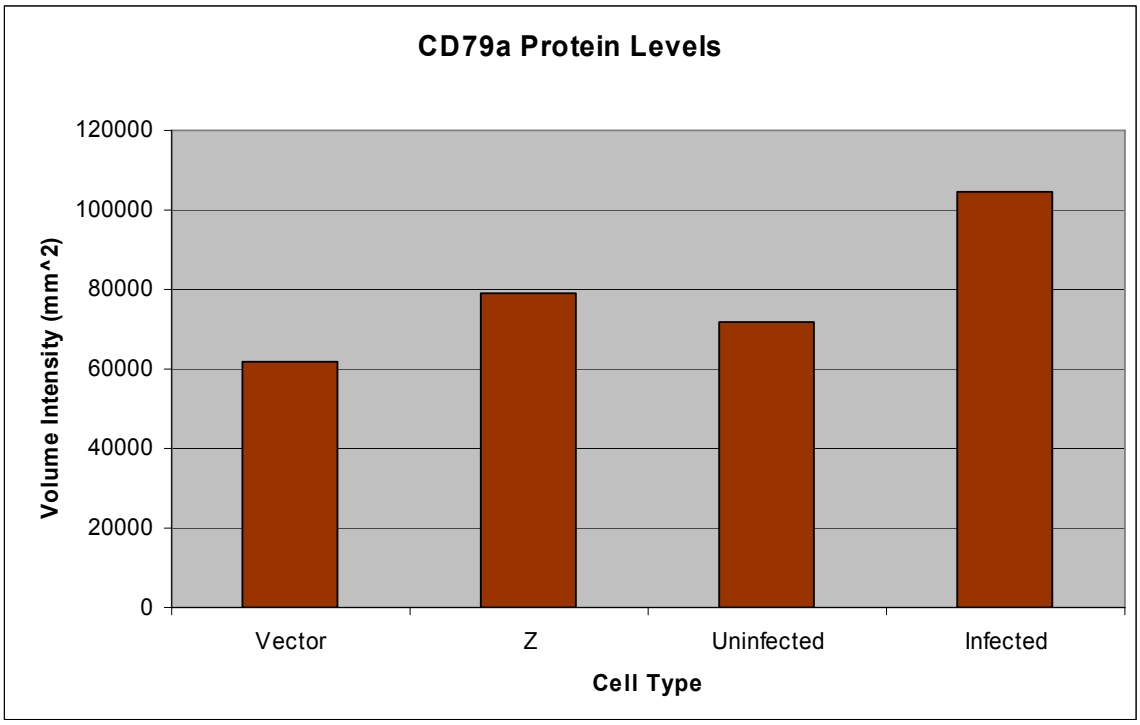

Figure 20: Quantification of Raji protein extract CD79a western blot. CD79a protein levels increase when cells are infected with EBV or are expressing BZLF1. Each bar represents a different condition 1) transfected with control vector (vector); 2) transfected with BZLF1 expression vector (Z); 3) EBV uninfected; and 4) EBV infected.

When comparing Raji cells transfected with control vector to those transfected with BZLF1 expression vector an increase in overall CD79a protein levels was detected. These results correspond to detection of CD79a by immunofluorescence (Figure 18). Overall the results indicate that there is an increase in CD79a during EBV lytic infection, and that the EBV specific protein BZLF1 can lead to increased CD79a levels.

c). CD19 protein expression levels determined by confocal microscopy:

The level of CD19 protein in BZLF1 expressing or EBV lytically replicating B cells was quantified by confocal microscopy. I transfected Raji cells with a control or BZLF1 expression plasmid. I also infected Raji B cells with the EBfaV-GFP virus, while also leaving a group of cells uninfected as a control. 48 hours post-transfection or post-infection, cells were stained through immunocytochemistry with an anti-CD19 antibody, as well as an anti-BZLF1 antibody for transfected cells. Cells were then examined by confocal microscopy and images of infected cells (GFP or BZLF1 staining) were taken (Figure 21). Uninfected and control vector transfected cells were also analyzed. These cells were then quantified using Fluoview confocal software to measure the levels of CD19 staining intensity from the four conditions listed (Figure 22).

Figure 21 shows images of all four conditions that were analyzed. CD19 expression is stained red, GFP or BZLF1 expression is stained green, and DNA is shown as blue. In the upper left panel is imaging of Raji cells uninfected with EBV. The CD19 protein levels were compared to the upper right panel showing cells infected with EBV. Only cells expressing the GFP tag were quantified, indicated by the arrow, as these were cells that are infected with EBV. The bottom left panel is imaging of Raji cells transfected with a control vector. The CD19 protein levels were compared to the bottom right panel showing cells transfected with a BZLF1 expression plasmid. Once again only cells expressing BZLF1, indicated by the arrow, were quantified. Using a GFP tag and staining for BZLF1 expression assured that only cells actually infected or transfected were quantified and used for comparison.

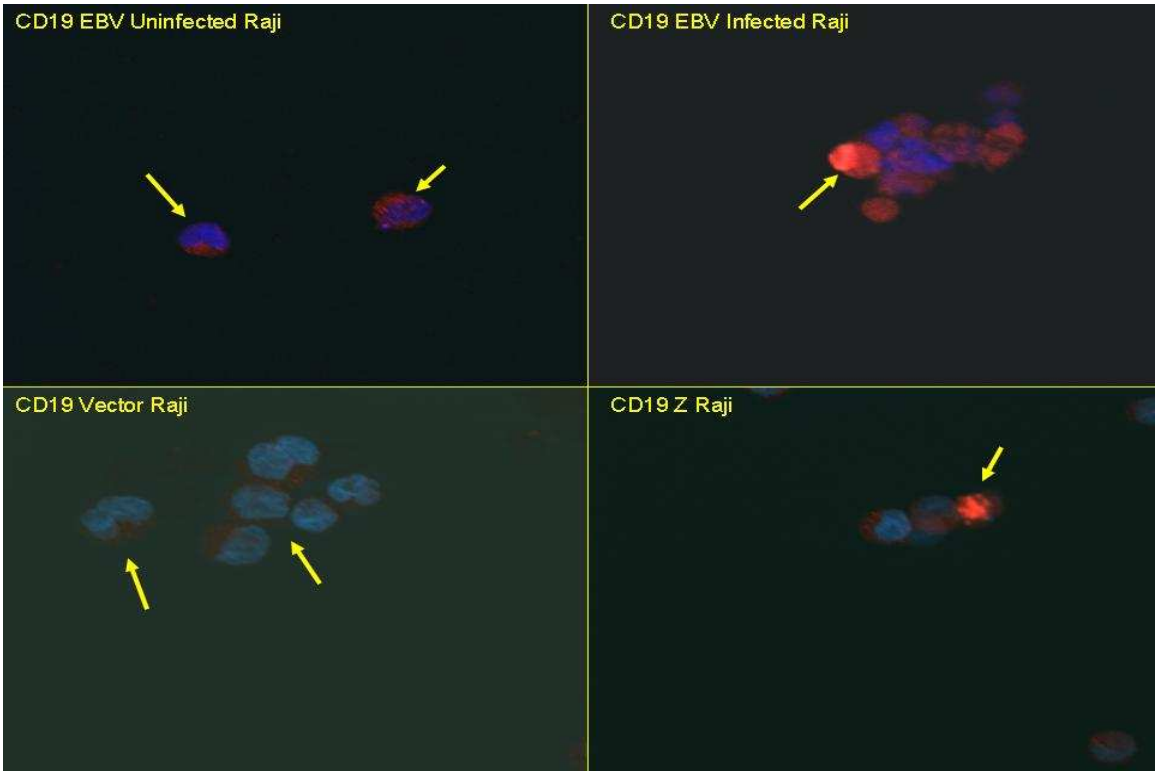

Figure 21: Confocal images of Raji cells, stained for CD19 (red), BZLF1/GFP expression (green) and DNA (blue). Arrows point to cells that were quantified. Four conditions are represented. EBV uninfected cells top left, EBV infected cells top right, vector transfected cells bottom left, BZLF1 transfected cells bottom right.

Figure 22 shows the quantification of the images seen in Figure 21. Each quantification is an average of at least 24 cells. Looking at CD19 protein levels, they appear to follow the same pattern that was seen while looking at CD79a protein levels. First, when cells were infected with EBV they have larger levels of CD19 in comparison to cells that were uninfected. Second, when cells were transfected with BZLF1 expression plasmid they have larger levels of CD19 then cells only transfected with a vector. These results show that B-cells infected with EBV have increased levels of CD19, most likely caused by the lytic associated protein BZLF1.

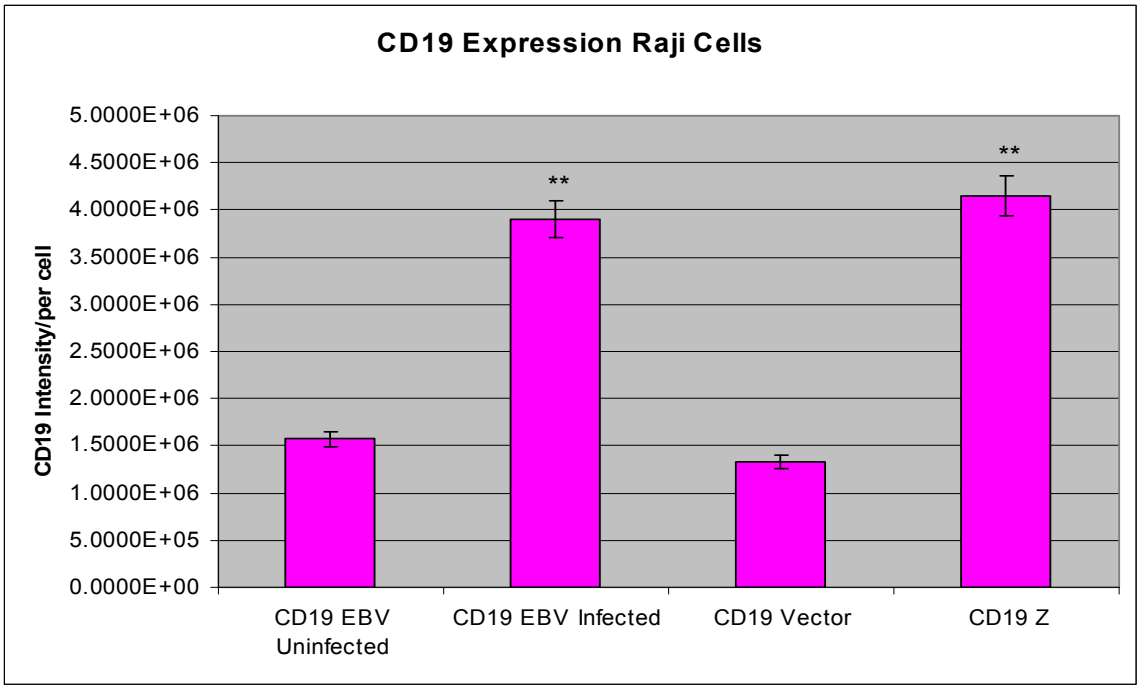

Figure 22: Average quantification of CD19 levels from confocal microscopy. CD19 protein levels increase when infected with EBV or in the presence of BZLF1. Four conditions shown, vector, BZLF1 expression, EBV uninfected, and EBV infected. ** $p<.0005$ (n=24)

d). CD19 protein expression levels determined by western blot analysis:

As before, in addition to immunocytochemistry, I performed Western blot analysis. Protein from the four conditions (BZLF1-transfected, control transfected, uninfected Raji, infected Raji) in equal amounts were run on an SDS-PAGE gel. These were then transferred to nitrocellulose, and immunoblot analysis was performed with an anti-CD19 antibody (Figure 23) and standardized using Actin. The bands from the four conditions were then quantified with quantitation software (Figure 24).

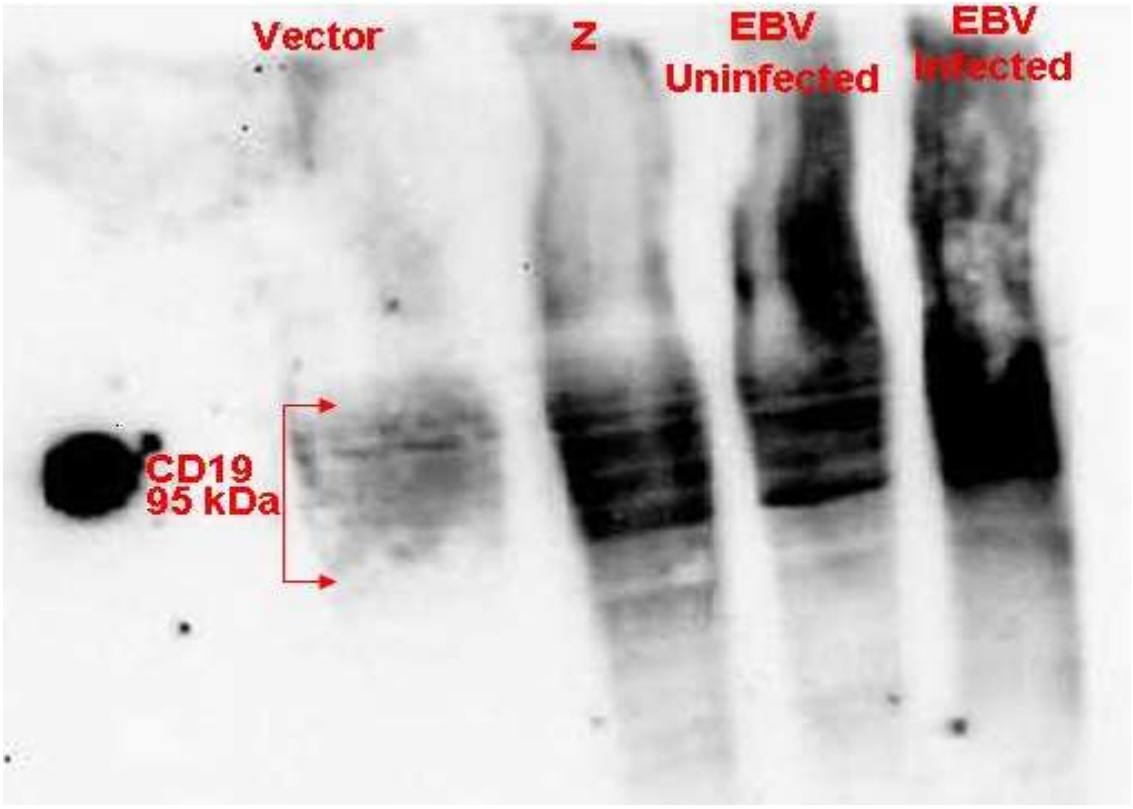

Figure 23: Western Blot of CD19 protein levels for varying transfection conditions showing increased CD19 with EBV infected or BZLF1 is expressed. The four conditions shown from Raji cells are 1) transfected with control vector (vector); 2) transfected with BZLF1 expression vector (Z); 3) EBV uninfected; and 4) EBV infected. CD19 is found at 95kDa.

The CD19 protein bands from Figure 23 are similar to the results seen in Figure 22 when analyzing through immunocytochemistry. There appeared to be less CD19 present when Raji cells were transfected with a control vector or uninfected with EBV. In contrast, when Raji cells were transfected with BZLF1 or infected with EBV there was an increase in CD19 protein. CD19 protein bands are normally found at 95kDa, but there are three major isoforms that were detected by the antibody, as shown in the figure. To quantify the CD19 protein levels all three bands were analyzed together (Figure 24).

When comparing the EBV uninfected cells to the EBV infected cells there appeared to be an increase in CD19 in the EBV infected cells (Figure 24). The increase in CD19 protein levels was also seen when comparing vector transfected Raji cells with BZLF1 expressing Raji cells. This increase was approximately 2 fold. These results match what was seen when analyzing CD19 protein levels through confocal imaging (Figure 22), as well as match the results seen when looking at CD79a protein levels (Figure 18 and 20).

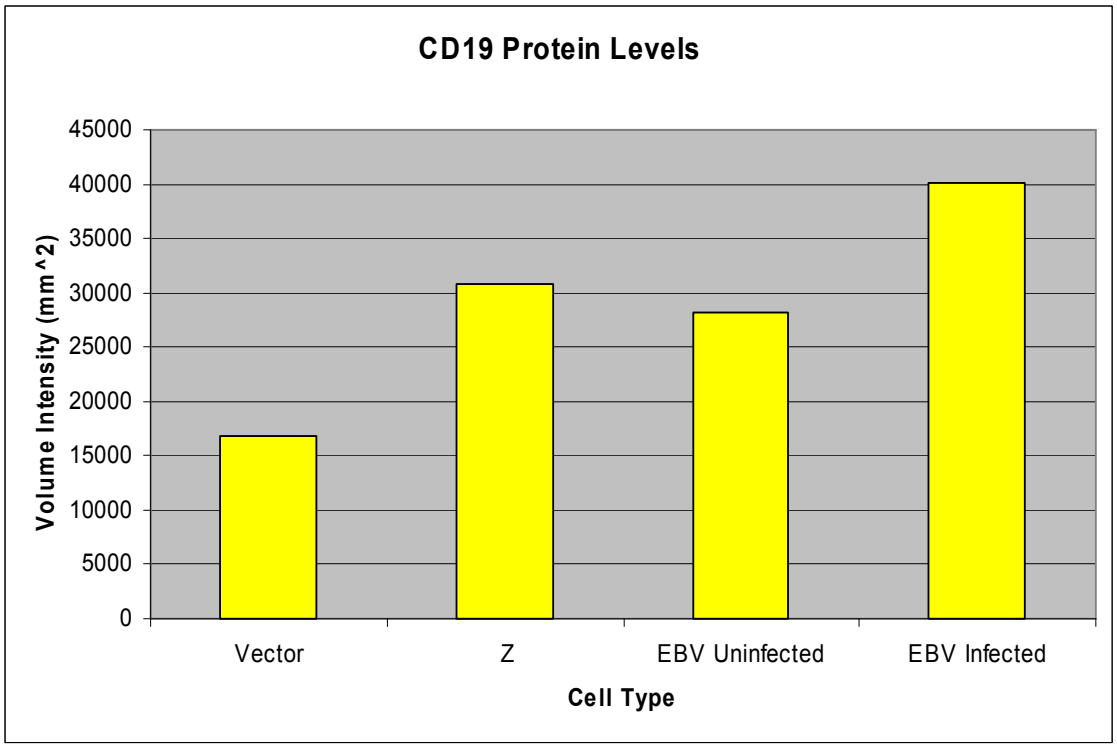

Figure 24: Quantification of Raji protein extract CD19 western blot. CD19 protein levels increase when cells are infected with EBV or are expressing BZLF1. Each bar represents a different condition 1) transfected with control vector (vector); 2) transfected with BZLF1 expression vector (Z); 3) EBV uninfected; and 4) EBV infected.

When examining both CD79a and CD19 protein levels in EBV infected Raji cells, both protein levels were significantly increased in comparison to uninfected cells. To ensure that this increase was caused by BZLF1, and more specifically BZLF1 and its ability to stabilize and increase Pax5 levels, protein levels of CD79a and CD19 were both examined in relation to BZLF1 transfected cells. As seen with EBV infected cells, BZLF1 expressing cells had a significant increase in CD79A and CD19 protein levels. These results indicate that when there were increased levels of Pax5 there were also increased protein levels of Pax5 transcriptional targets CD79a and CD19. These results were expected, as the more Pax5 and the longer it stays active, the more likely transcriptional targets will be turned on. These results were extremely interesting in that they may be applied to certain leukemias where CD19 and CD79a levels are found altered.

CHAPTER IV

DISCUSSION

The Epstein-Barr virus has been shown to have the ability to affect cellular integrity through a variety of actions. One such action is through the binding of the lytic protein BZLF1 to cellular host proteins. BZLF1 has been well documented in its ability to physically interact with p53, CBP, PML, c-Jun N-terminal kinases, and p38. (Adamson et al 2000; Adamson and Kenney 2001; Adamson et al. 2005). Here I describe several effects of BZLF1 and its physical interaction with Pax5, a relatively unknown interaction. I have shown that the presence of BZLF1 increased Pax5 protein levels, presumably by stabilizing the Pax5 protein. BZLF1 has been previously shown to physically interact with PML and p53, and this physical interaction led to an increase in p53 and PML protein levels by stabilization of the protein (Mauser et al. 2002; Bowling and Adamson 2006). My data showing no changes in Pax5 mRNA levels provides further support that protein stabilization leads to the increase in Pax5 protein in cells expressing BZLF1 and that the BZLF1/Pax5 complex stabilizes the Pax5 protein. The mechanism for increased stabilization is not known, but most likely the BZLF1 protein with a long half-life, shelters the Pax5 protein from normal degradation.

The increase in Pax5 protein levels showed no detrimental effect to EBV lytic replication. In fact, it is hypothesized that BZLF1 physical interaction with Pax5 may aid

in the establishment of the EBV lytic cycle. Pax5 normally aids in the establishment of the EBV latent cycle through the activation of the latent promoter Wp (Tierney et al 2000). It is hypothesized that the physical interaction of BZLF1 with Pax5 may prevent Pax5 from properly activating the latent promoter Wp. This hypothesis still needs to be tested, but would establish a functional reason for the physical interaction between BZFL1 and Pax5.

Like most cellular manipulations, the increase in Pax5 protein levels results in a cascade of cellular changes. Overexpression of Pax5 has been seen in almost all non-Hodgkin lymphomas, and simple mutations to Pax5 are associated with Burkitt's lymphoma. One unique change that I documented was the increase in histone-H3 lysine-9 methylation levels. Pax5 is a multi-functional protein in that it is essential for the establishment of B-cell identity. One function of Pax5 is its ability to promote V_H to D_HJ_H gene arrangement through the loss of histone-H3 lysine-9 methylation in the V_H locus (Johnson et al. 2004). Through demethylation of the H3 lysine, Pax5 allows the B-cell recombinase machinery access to DNA (Johnson et al. 2004). The ability of Pax5 to act as an epigenetic modifier was examined in relation to its binding to BZLF1.

Previous studies have demonstrated that proteins bound to BZLF1 retain some of their functional ability. For example, when BZLF1 physically binds to CBP, and this complex then binds to mitotic chromosomes, there is an increase in levels of acetylated histone H3 (Adamson, 2005). CBP is a known histone acetylase that acts to acetylate histones in chromatin so it is expected that there should be a rise in histone acetylation levels. Reasoning would then suggest that the binding of the BZLF1/Pax5 complex to

mitotic chromosomes would result in the demethylation of histone H3 through the histone demethylase activity of Pax5. I have demonstrated that this is actually not the case, and instead histone H3 methylation levels increased when BZLF1 interacts with Pax5.

Transfections of D98/HE-R1 cells, which do not naturally produce Pax5, were used. This provided for the three control conditions of vector, Pax5 alone, and BZLF1 alone to be established. This assured that the results seen in the condition BZFL1 and Pax5 together were the result of only the interaction between the two and not each as individuals. As seen in Figure 16 when Pax5 was alone, as expected, the histone H3 methylation levels dropped as Pax5 acted as a histone demethylase. When BZLF1 and the vector were alone, the methylation levels stayed constant or rose slightly. The BZLF1 protein contains many different epigenetic properties including acting as a DNA and histone methylase (Bhende et al. 2004).

When BZLF1 and Pax5 were present together, there was an increase in histone-H3 lysine-9 methylation levels. This increase in methylation levels may be attributed to the binding of the BZLF1/Pax5 complex to chromosomes. Since Pax5 is a demethylase and BZLF1 is a methylase, a logical explanation is that the BZLF1/Pax5 complex binds to chromosomes exposing the active methylase subunit of the BZLF1 protein to the chromatin. However, one can not assume that this is the case and further investigation is warranted.

It is unknown if this increase in histone H3 methylation is simply a byproduct of the BZLF1/Pax5 interaction or if it serves a greater purpose within EBV lytic replication. Histone hypermethylation often corresponds with DNA hypermethylation and both

correspond with gene silencing. This is especially apparent in cancer where promoter CpG island hypermethylation of tumor-suppressor genes is common (Esteller 2007). Specifically within EBV infected cells, epigenetic marks have been manipulated within cancers associated with EBV. For example the gene promoter of p73, a tumor suppressor, is methylated in gastric carcinoma only when in association with EBV (Ushiku et al. 2006). This occurrence furthers the need to investigate how the BZLF1/Pax5 complex leads to histone hypermethylation.

Future experiments should focus on the actual BZLF1/Pax5 complex and what protein domains are exposed and how it binds to the mitotic chromosomes of the infected cell. This may shed light on how the BZLF1/Pax5 complex leads to hypermethylation of histone H3. Furthermore, a look at specific tumor suppressor genes associated with EBV cancers must be examined in relation to their epigenetic marks, and whether these marks may correspond with hypermethylation of histone H3. Indirectly, the BZLF1/Pax5 complex may be contributing to tumorgenesis associated with EBV. This is especially true as effects on chromosomes by BZLF1 may occur in cells that do not lyse to release viral particles. This is seen in tumors such as NPC where BZLF1 may be expressed but an incomplete lytic cycle is established, and the intracellular effects of BZLF1 prolonged (Martel-Renoir et al. 1995).

Another important function of Pax5 is its ability to transactivate B-cell specific genes including *CD19*, *blk*, *CD79a*, and *RAG-2*, while also repressing the genes *perforin*, *GATA-1*, *M-CSF-R*, and *Notch1*. Pax5 function as both a transcriptional repressor and activator depends on interactions with positive regulators like the TATA-binding protein

or corepressors of the Groucho protein family (Nutt 2001). With so many genes dependent on Pax5 function I examined how the increased levels of Pax5 protein, caused by the Pax5/BZLF1 complex, affected Pax5 targets.

The two Pax5 target genes examined were *CD79a* and *CD19*. Within B cells the antigen receptor complex includes surface immunoglobin (Ig), which non-covalently associates with Ig-alpha and Ig-beta, both necessary for B-cell antigen receptor function and expression. CD79a is the Ig-alpha component of this antigen receptor complex. CD19 is a cell surface protein that functions as a general control for antigen receptor-induced signaling thresholds, which are critical for development of the B cell pool and humoral immunity. CD19 also links humoral immune responses with innate immune response through association with the CD21 receptor (Tedder 2005). Both proteins play critical roles in B-cell function and development.

I have shown that an increase in levels of Pax5 protein are correlated with increased levels of Pax5 targets CD19 and CD79a. This increase in CD19 and CD79a is indirectly linked to the expression of the EBV lytic protein BZLF1. With the expression of BZFL1 and the stabilization of Pax5 there is an increase in Pax5 levels and therefore an increase in CD19 and CD79a activation. The increase in CD19 and CD79a proteins related to increased levels of Pax5 has been documented before when Cozman et al. examined overexpression of Pax5 through Myc5-M5 and Myc-M12 cells expressing the fusion of Pax5 and tamoxifen receptor (Cozma et al. 2007).

The overexpression of CD19 and CD79a is detrimental to B-cell development and function. B cell activation resulting from increases in CD19 expression or signaling

through the CD19 pathway predispose individuals to systemic autoimmunity and autoantibody production (Tedder 2005). Constitutive overexpression of CD19 on B cells also results in decreased numbers of B cells, hyper-responsiveness with greater antigen-presenting abilities, and increases in CD4+ and CD8+ levels (Stohl 2005). CD79a has been implemented as a major component in overexpression of Pax5 resulting in neoplastic growth through B-cell receptor signaling (Cozman et al. 2007).

Both CD19 and CD79a are integral components of B-cell development. I propose that the increase in Pax5 levels I have shown in EBV infected cells results in the increase in CD19 and CD79a I have also shown. Changes to these two critical B-cell components results in a variety of intercellular changes (Cozman et al. 2007). These changes have been associated with many different cancers, and more specifically cancers associated with EBV. This correlation warrants a further investigation into how CD19 and CD79a levels are increasing when Pax5 interacts with BZLF1. Further experiments need to be conducted to determine if other Pax5 transcriptional targets are affected. Since Pax5 is such a multifunctional protein, changes to Pax5 may result in even more cellular changes beyond what is mention in this study.

CHAPTER V

CONCLUSION

EBV is one of the most prevalent viruses in the world, and once infected, the virus remains with a person for life. Though initial infection is typically harmless, infection has been associated with a variety of cancers. For this reason, it is essential to determine how EBV manipulates its cellular host to survive. Any changes in normal cellular activity could be an underlying cause of cancers associated with the virus. In this study, I have demonstrated that infection by lytically replicating EBV results in increased levels of Pax5. Since Pax5 is such a multifunctional protein within B-cell development this increase in Pax5 levels results in many cellular changes to infected cells. Associated with increased levels of Pax5 is an increase in histone-H3 lysine-9 methylation levels as well as an increase in CD19 and CD79a protein levels.

These increases, as mentioned, have significant consequences for normal B-cell function and development. Many of the resulting consequences can be linked back to underlying causes of cancer. The establishment of this link furthers the need to examine Pax5 and its relation to changes associated with EBV infected cells. Since Pax5 does have so many functions, and it has now been shown that Pax5 is significantly altered in EBV infected cells, other Pax5 targets and functions must be examined. In the end, Pax5 is only one protein manipulated by EBV for survival and replication of the virus

However, it strongly demonstrates how this manipulation results in serious intracellular consequences for EBV infected cells

REFERENCES

Adamson, A.L., 2005 The Epstein-Barr virus BZLF1 protein associates with mitotic chromosomes. J. Virol. 79: 7899-7904.

Adamson, A.L., and S. Kenney, 1999 The Epstein-Barr virus BZLF1 protein interacts physically and functionally with the histone acetylase CREB-binding protein. J. Virol. 73: 6551-6558.

Adamson, A., and S. Kenney, 2001 The Epstein-Barr Virus (EBV) immediate-early protein, BZLF1 is SUMO-1-modified and disrupts PML bodies. J. Virol. 75: 2388-2399.

Adamson, A., D. Darr, E. Holley-Guthrie, R.A. Johnson, A. Mauser et al., 2000 Epstein-Barr virus immediate-early proteins BZLF1 and BRLF1 activate the ATF2 transcription factor by increasing the levels of phosphorylated p38 and c-Jun N-terminal kinases. J. Virol. 74: 1224-1233.

Adamson, A., N Wright, and D. Lajeunesse, 2005 Modeling early Epstein-Barr Virus infection in Drosophila melanogaster, the BZLF1 protein. Genetics 171: 1125-1135.

Bhende, P., W. Seaman, H.J. Delecluse, and S. Kenney, 2004 The EBV lytic switch protein, Z, preferentially binds to an activates the methylated viral genome. Nature Genetics 10: 1099-1104.

Bowling, B., and A. Adamson, 2006 Functional interactions between the Epstein-Barr Virus BZLF1 protein and the promyelocytic leukemia protein. Virus Research. 117: 244-253.

Burkhardt, A., M. Brunswick, J. Bolen, and J. Mond, 1991 Anti-immunoglobulin stimulates B lymphocytes activates src-related protein-tyrosine kinases. Proc. Natl. Acad. Sci 88: 7410-7414.

Calame, K.L., K.I. Lin and C. Tunyaplin, 2003 Regulatory mechanisms that determine the development and function of plasma cells. Annu. Rev. Immunol. 21: 205-230.

Chevallier-Greco, A., E. Manet, P. Chavrier, C. Mosnier, J. Daillie et al,. 1986 Both Epstein-Barr virus (EBV) encoded trans-acting factors, EB1 and EB2, are required to activate transcription from an early EBV promoter. EMBO J. 5: 3243-3249.

Cobaleda, C., A. Schebesta, A. Delogu, and M. Busslinger, 2007 Pax5: the guardian of B cell identity and function. Nature Immunology 8(5):463-470.

Cozma, D., Y. Duonan, S. Hodawadeker, A. Azvolinsky et al. 2007 B cell activator Pax5 promotes lymphomagenesis through stimulation of B-cell receptor signaling. JCI 117:2602-2610

Engel, P., L.J. Zhou, D. Ord, S. Sato, B. Koller, and T. Tedder, 1995 Abnormal B lymphocyte development, activation, and differentiation in mice that lack or overexpress the CD19 signal transduction molecule. Immunity 3: 39-50.

Enver, T., 1999 B-Cell commitment: Pax5 is the deciding factor. Curr. Biol. 9: R933-R935.

Esterller, M. 2007 Epigenetic gene silencing in cancer: the DNA hypermethylome. Hum. Mol. Genet. 1: R50-9.

Giot, J.F, I. Mikaelian, M. Duisson, E. Mane, I. Joab et al., 1991 Transcriptional synergy and interference between the EBV transcription factors EB1 and R require both the basic region and the activation domains of EB1. Nucleic Acids Res. 19: 1251-1258.

Glaser, R. and F.J. O'neill. 1972 Hybridization of Burkitt lymphoblastoid cells. Science 176: 1245-1247.

Johnson, K., D. Pflugh, D. Yu, D. Hesslein, K.I., Lin, et al. 2004 B cell-specific loss of histone 3 lysine 9 methylation in the Vh locus depends on Pax5. Nat. Immunol. 5: 853-861.

Kenney, S., E. Holley-Guthrie, E.-C. Mar and M. Smith, 1989 The Epstein-Barr virus BMLF1 promoter contains an enhancer element that is responsive to the BZLF1 and BRLF1 transactivators. J. Virol. 63: 3878-3883.

Kishi, H.K., X. Wei, Z. Jin, Y. Fujishiro, T. Nagata et al. 2000 Lineage-specific regulation of the murine Rag-2 promoter: GATA-3 in T cells and Pax-5 in B cells. Blood 95: 3845- 3852.

Krenacs, L., et al. 1998 Transcription factor B-cell specific activator protein (BSAP) is differentially expressed in B-cells and in subsets of B-cell lymphomas. Blood 92:1308-1316.

Marte-Renoir, D., V. Grunewalkd, R. Touitou, G. Schwaab, and I. Joab, 1995 Qualitative analysis of the expression of Epstein-Barr virus lytic genes in nasopharyngeal carcinoma biopsies. J. Gen. Virol. 76:1401-1408

Mason, D., J. Cordell, M. Brown, J. Borst, M. Jones, et al., 1995 CD79a: A novel marker for B-cell neoplasms in routinely processed tissue samples. Blood 86: 1453-1459.

Mauser, A., S. Saito, E. Appella, C.W. Anderson, W.T Seaman, et al., 2002. The Epstein-Barr virus immediate-early protein BZLF1 regulates p53 function through multiple mechanisms. J. Virol. 76: 12503-12512.

Nutt, S.L, D. Eberhard, M. Horcher, A.G. Rolink and M. Busslinger, 2001 Pax5 determines the identity of B cells from the beginning to the end of B-lymphopoiesis Int. Rev. Immunol. 20 (1):65-82.

Nguyen, C.T., D. Weisenberger, M. Velicescu, F. Gonzales, J. Lin, G. Liang, and P. Jones, 2002 Histone H3-Lysine 9 methylation is associated with aberrant gene silencing in cancer cells and is rapidly reversed by 5-Aza-2'-deoxycytidine. Cancer Research 62: 6456-6461.

Quinlivan, E., E. Holley-Guthrie, M. Norris, D. Gutsch, S. Bachenheimer et al., 1993 Direct BRLF1 binding is require for cooperative BZLF1/BRLF1 activation of the Epstein-Barr virus early promoter, BMRF1. Nucleic Acids Res. 21: 1999-2007.

Rickinson, A, 2002 Epstein - Barr virus. Virus Research 82: 109-113.

Sambrook, J., E.F. Fritsch, and T. Maniatis, 1989 *Molecular Cloning: A Laboratory Manual*, Ed. 2. Cold Spring Harbor Laboratory Press, Cold Spring Harbor, NY.

Schelcher, C., S. Valencia, H.J. Delecluse, M. Hicks, and A. Sinclair, 2005 Mutation of a single amino acid residue in the basic region of the Epstein-Barr Virus (EBV) lytic cycle switch protein Zta (BZLF1) prevents reactivation of EBV from latency. J. Virol. 79: 13822-13828.

Speck, P. and R. Longnecker. 1999 Epstein-Barr virus (EBV) infection visualized by EGFP expression demonstrates on known mediators of EBV entry. Arch. Virol. 144: 1123-1137.

Stohl, W., X. Dong, K.S. Kim, T.F. Tedder, S. Sato, Humoral autoimmunity in mice overexpressing B cell surface CD19: Vital role for MHC class II. Clinical Immunology 116 (3):257-264

Tedder, T.F, J.C. Poe, M. Fujimoto, K.M. Haas, and S. Sato, 2005 The CD19-CD21 Signal Transduction Complex of B Lymphocytes Regulates the Balance between Health and Autoimmune Disease: Systemic Sclerosis as a Model System. Karger 80:55-90.

Tierney, R.J., H.E. Kirby, J.K. Nagara, J. Desmond, A.I. Bell et al., 2000 Methylation of transcription factor binding sites in the Epstein-Barr virus latent cycle promoter Wp coincides with promoter down-regulation during virus-induces B-cell transformation. J. Virol. 74: 10468-10479.

Ushku, T., J.M. Chong, H. Uozaki, R. Hino, M.S. Chang et al., 2006 p73 gene promoter methylation in Epstein-Barr virus-associated gastric carcinoma. Int. J. Cancer 120: 60-66.

Zhang, Q,. D. Gutsch and S. Kenney, 1994 Functional and physical interaction between p53 and BZLF1: implications for Epstein Barr virus latency. Mol. Cell. Biol. 14: 1929-1938.